SOI: 1.1/TAS DOI: 10.15863/TAS

International Scientific Journal

Theoretical & Applied Science

p-ISSN: 2308-4944 (print) **e-ISSN:** 2409-0085 (online)

Year: 2023 **Issue:** 05 **Volume:** 121

Published: 28.05.2023 **http://T-Science.org**

Issue Article

Denis Chemezov
Vladimir Industrial College
M.Sc.Eng., Academician of International Academy of
Theoretical and Applied Sciences, Lecturer, Russian Federation
https://orcid.org/0000-0002-2747-552X
vic-science@yandex.ru

Sergey Prokopenko
Vladimir Industrial College
Student, Russian Federation

Mikhail Chebotaryov
Vladimir Industrial College
Student, Russian Federation

Anton Ilin
Vladimir Industrial College
Student, Russian Federation

Dmitriy Netsvetaev
Vladimir Industrial College
Student, Russian Federation

Aleksandr Cheryomushkin
Vladimir Industrial College
Student, Russian Federation

Danil Sukhorukov
Vladimir Industrial College
Student, Russian Federation

REFERENCE DATA OF PRESSURE DISTRIBUTION ON THE SURFACES OF AIRFOILS HAVING THE NAMES BEGINNING WITH THE LETTER S (THE SECOND PART)

***Abstract**: The results of the computer calculation of air flow around the airfoils having the names beginning with the letter S (continuation) are presented in the article. The contours of pressure distribution on the surfaces of the airfoils at angles of attack of 0, 15 and -15 degrees in conditions of the subsonic airplane flight speed were obtained.*

***Key words**: airfoil, angle of attack, pressure, surface.*

***Language**: English*

***Citation**: Chemezov, D., et al. (2023). Reference data of pressure distribution on the surfaces of airfoils having the names beginning with the letter S (the second part). *ISJ Theoretical & Applied Science, 05 (121),* 532-584.

Soi: http://s-o-i.org/1.1/TAS-05-121-59 ***Doi***: crossref https://dx.doi.org/10.15863/TAS.2023.05.121.59

***Scopus ASCC**: 1507.*

Introduction

Creating reference materials that determine the most accurate pressure distribution on the airfoil surfaces is an actual task of the airplane aerodynamics.

Materials and methods

The study of air flow around the airfoils was carried out in a two-dimensional formulation by means of the computer calculation in the *Comsol Multiphysics* program. The airfoils in the cross section were taken as objects of research [1-34]. In this work, the airfoils having the names beginning with the letter *S* were adopted. Air flow around the airfoils was carried out at angles of attack (α) of 0, 15 and -15 degrees. Flight speed of the airplane in each case was subsonic. The airplane flight in the atmosphere was carried out under normal weather conditions. The geometric characteristics of the studied airfoils are presented in the Table 1. The geometric shapes of the airfoils in the cross section are presented in the Table 2.

Table 1. The geometric characteristics of the airfoils.

Airfoil name	Max. thickness	Max. camber	Leading edge radius	Trailing edge thickness
SB96 10.5/3.0	10.39% at 31.6% of the chord	3.09% at 48.6% of the chord	0.5929%	0.0%
SB96 11.6/3.0	11.49% at 29.3% of the chord	3.09% at 51.3% of the chord	0.7363%	0.0%
SB96 LM 8/3.0	8.05% at 33.0% of the chord	2.99% at 37.2% of the chord	0.5548%	0.0%
SB96 MU 8.5/1.73	8.5% at 28.2% of the chord	1.73% at 40.9% of the chord	0.6053%	0.0%
SB96V 9.35/1.25	9.35% at 30.1% of the chord	1.25% at 50.4% of the chord	0.5047%	0.0%
SB96VS 9.75/1.25	9.74% at 35.9% of the chord	1.25% at 39.7% of the chord	0.6269%	0.0392%
SB97 FW 8.93/2	8.91% at 28.1% of the chord	2.01% at 32.6% of the chord	0.823%	0.1959%
SB97EP 9.2/1.9	9.29% at 29.5% of the chord	1.9% at 38.2% of the chord	0.7837%	0.14%
SB97EPW 8/2	8.03% at 27.9% of the chord	2.01% at 40.5% of the chord	0.6026%	0.1206%
SB98F3J 8/3.5	7.99% at 28.6% of the chord	3.51% at 41.2% of the chord	0.5549%	0.1206%
SBC3	11.21% at 29.3% of the chord	2.98% at 38.9% of the chord	1.1393%	1.0%
SC(2)-0714 Supercritical airfoil	13.93% at 37.0% of the chord	1.48% at 80.0% of the chord	2.3468%	0.59%
SD2030	8.56% at 35.2% of the chord	2.25% at 45.7% of the chord	0.5963%	0.049%
SD2030-086-88	8.56% at 35.2% of the chord	2.25% at 45.7% of the chord	0.678%	0.0%
SD2083 (9,0%)	8.96% at 35.2% of the chord	2.84% at 45.7% of the chord	0.6395%	0.0%
SD5060 (9,5%)	9.46% at 24.9% of the chord	2.29% at 45.2% of the chord	0.849%	0.0%
SD6060-104-88	10.35% at 36.3% of the chord	1.84% at 36.3% of the chord	0.6673%	0.0%
SD6060-104-88~1	10.35% at 36.3% of the chord	1.84% at 36.3% of the chord	0.6673%	0.0%
SD6080 (9,2%)	9.16% at 28.9% of the chord	3.73% at 39.2% of the chord	0.7431%	0.0%
SD7003	8.52% at 25.8% of the chord	1.46% at 35.5% of the chord	0.8189%	0.02%
SD7003-085-88	8.5% at 25.7% of the chord	1.45% at 35.4% of the chord	0.7909%	0.0%
SD7032	9.99% at 28.2% of the chord	3.66% at 43.9% of the chord	0.9926%	0.204%
SD7032-099-88	9.95% at 28.2% of the chord	3.65% at 43.7% of the chord	0.7508%	0.0%
SD7034	10.51% at 28.3% of the chord	3.88% at 38.6% of the chord	0.9141%	0.0%
SD7037	9.2% at 29.1% of the chord	3.01% at 39.3% of the chord	0.8039%	0.0%
SD7043 (9,1%)	9.13% at 28.1% of the chord	3.5% at 49.2% of the chord	0.791%	0.0%
SD7062 (14%)	13.98% at 27.2% of the chord	3.96% at 37.2% of the chord	1.6404%	0.0%
SD7080 (9,2%)	9.15% at 29.7% of the chord	2.48% at 39.9% of the chord	0.7575%	0.0%
SD7084 (9,6%)	9.62% at 30.5% of the chord	2.3% at 35.5% of the chord	0.7163%	0.0%
SD7090 (10%)	9.97% at 30.1% of the chord	1.86% at 35.1% of the chord	0.9577%	0.0%
SD8000	8.88% at 25.6% of the chord	1.72% at 45.7% of the chord	0.8258%	0.021%
SD8000-089-88	8.85% at 25.5% of the chord	1.71% at 45.6% of the chord	0.8152%	0.0%
SD8020	10.1% at 27.5% of the chord	0.0% at 0.0% of the chord	0.8334%	0.0%
SD8020-010-88	10.1% at 27.5% of the chord	0.0% at 57.6% of the chord	0.8334%	0.0%
SD8040	10.03% at 29.4% of the chord	2.66% at 39.6% of the chord	1.2573%	0.023%
SD8040 (10%)	10.0% at 29.3% of the chord	2.65% at 39.5% of the chord	1.2028%	0.0%
SELIG 3002-099-83	9.93% at 28.7% of the chord	2.99% at 38.8% of the chord	1.1201%	0.0%
SG 6040	16.0% at 35.5% of the chord	2.5% at 58.2% of the chord	1.3278%	0.0%
SG 6041	9.99% at 37.9% of the chord	2.0% at 37.9% of the chord	0.8659%	0.0%
SG 6042	9.99% at 35.1% of the chord	3.75% at 47.1% of the chord	1.1875%	0.0%
SG 6043	10.01% at 32.3% of the chord	5.49% at 48.8% of the chord	1.4784%	0.0%
SG6050	16.02% at 31.8% of the chord	3.24% at 47.4% of the chord	1.2362%	1.0%
SG6051	12.0% at 36.8% of the chord	3.22% at 48.9% of the chord	0.7361%	1.0%
SH-6457	6.9% at 20.0% of the chord	7.35% at 40.0% of the chord	0.8131%	0.85%
SHUCOSKJ	11.53% at 20.0% of the chord	7.05% at 40.0% of the chord	1.923%	0.0%
SI33006	6.0% at 30.0% of the chord	3.0% at 30.0% of the chord	1.3041%	0.0%
SI53507	7.1% at 20.0% of the chord	5.15% at 30.0% of the chord	1.4377%	0.3%
SI-63008	7.1% at 20.0% of the chord	5.15% at 30.0% of the chord	1.4425%	0.2%
SIKORSKY DBLN-526	25.99% at 50.0% of the chord	3.99% at 50.0% of the chord	3.0502%	0.0%
SIKORSKY GS-1	13.9% at 30.0% of the chord	4.14% at 50.0% of the chord	2.0797%	0.0%

SIKORSKY SC1012R8	12.0% at 27.6% of the chord	2.71% at 21.5% of the chord	2.801%	0.4368%
SIKORSKY SC1094 R8	9.4% at 27.6% of the chord	2.12% at 21.6% of the chord	1.7042%	0.3423%
SIKORSKY SC1094R8	9.5% at 26.9% of the chord	0.81% at 26.9% of the chord	2.5708%	0.34%
SIKORSKY SC1095	9.5% at 26.9% of the chord	0.81% at 26.9% of the chord	0.7644%	0.3458%
SIKORSKY SC2110	9.93% at 37.7% of the chord	1.96% at 15.7% of the chord	1.1578%	0.3575%
SIKORSKY SSC-A07	7.0% at 37.7% of the chord	0.91% at 17.2% of the chord	0.4056%	0.2497%
SIKORSKY SSC-A09	9.0% at 37.7% of the chord	1.17% at 17.2% of the chord	0.6896%	0.321%
SIMPLEX1	0.99% at 40.0% of the chord	0.49% at 40.0% of the chord	0.7041%	0.0%
SIMPLEX2	1.99% at 40.0% of the chord	1.0% at 40.0% of the chord	0.6426%	0.0%
SIMPLEX3	2.98% at 40.0% of the chord	1.49% at 40.0% of the chord	0.5744%	0.0%
SIMPLEX4	3.98% at 40.0% of the chord	1.99% at 40.0% of the chord	0.5099%	0.0%
SIMPLEX5	4.97% at 40.0% of the chord	2.48% at 40.0% of the chord	0.4787%	0.0%
SIMPLEX6	5.97% at 40.0% of the chord	2.98% at 40.0% of the chord	0.5641%	0.0%
SIMPLEX7	6.96% at 40.0% of the chord	3.48% at 40.0% of the chord	0.6483%	0.0%
SIMPLEX8	7.96% at 40.0% of the chord	3.98% at 40.0% of the chord	0.7393%	0.0%
SIMPLEX9	8.95% at 40.0% of the chord	4.47% at 40.0% of the chord	0.8728%	0.0%
Sipkill 1,7/10	9.88% at 29.9% of the chord	1.68% at 29.9% of the chord	0.6907%	0.0%
SL 1	12.95% at 30.0% of the chord	6.85% at 40.0% of the chord	1.9796%	0.7%
SL-1	12.95% at 30.0% of the chord	6.85% at 40.0% of the chord	1.1839%	0.7%
SLOTFLAP	18.04% at 25.3% of the chord	1.42% at 35.2% of the chord	0.7301%	0.26%
SM8016m	7.99% at 26.0% of the chord	1.6% at 32.7% of the chord	0.6547%	0.2%
SM8516m	8.5% at 26.0% of the chord	1.6% at 32.7% of the chord	0.7407%	0.2%
Smoothed ATR airfoil coordinates obtained using A	14.51% at 24.6% of the chord	2.87% at 21.5% of the chord	1.8949%	0.0%
SOAVE-61	6.4% at 25.0% of the chord	7.4% at 40.0% of the chord	0.9317%	0.5%
SOKOLOV	7.1% at 25.0% of the chord	6.45% at 50.0% of the chord	0.7336%	0.7%
SPICA	11.7% at 30.0% of the chord	4.74% at 35.0% of the chord	1.2584%	0.0%
SPICA 11,73% smoothed	11.72% at 30.0% of the chord	4.74% at 35.0% of the chord	1.3008%	0.0%
SPICAM1	12.8% at 30.0% of the chord	4.21% at 35.0% of the chord	1.07%	0.0%
ST CYR 171 (ROYER)	11.08% at 30.0% of the chord	0.0% at 0.0% of the chord	1.5136%	0.0%
ST CYR 172 (ROYER)	13.56% at 30.0% of the chord	0.0% at 0.0% of the chord	1.9813%	0.0%
ST CYR 24	12.35% at 30.0% of the chord	7.4% at 40.0% of the chord	2.272%	0.0%
STCYR117	12.05% at 30.0% of the chord	6.03% at 30.0% of the chord	2.2549%	0.0%
STCYR171	11.08% at 30.0% of the chord	0.0% at 0.0% of the chord	1.5136%	0.0%
STCYR172	13.56% at 30.0% of the chord	0.0% at 0.0% of the chord	1.9813%	0.0%
STCYR234	16.0% at 20.0% of the chord	8.6% at 40.0% of the chord	3.2415%	0.0%
STCYR-24	12.35% at 30.0% of the chord	7.4% at 40.0% of the chord	2.272%	0.0%
STCYR-34	8.03% at 20.0% of the chord	4.66% at 30.0% of the chord	1.5255%	0.0%
STCYR-52	10.0% at 30.0% of the chord	5.0% at 30.0% of the chord	1.4529%	0.0%
STCYR-53	7.93% at 40.0% of the chord	4.54% at 30.0% of the chord	1.6634%	0.0%
STCYR-56	13.81% at 20.0% of the chord	7.6% at 40.0% of the chord	2.2993%	0.4%
STCYR-58	7.0% at 30.0% of the chord	0.0% at 0.0% of the chord	1.6787%	0.0%
STRAND	15.44% at 26.3% of the chord	4.08% at 31.9% of the chord	1.9843%	0.0%

Note:
SBC3 (profil pour aile en poly non coffre);
Sipkill 1,7/10 (is for Combat and nothing else!);
SL 1 (Italy);
ST CYR 171 (ROYER) (St. Cyr (France));
ST CYR 172 (ROYER) (St. Cyr (France));
ST CYR 24 (ST. CYR (France)).

Table 2. The geometric shapes of the airfoils in the cross section.

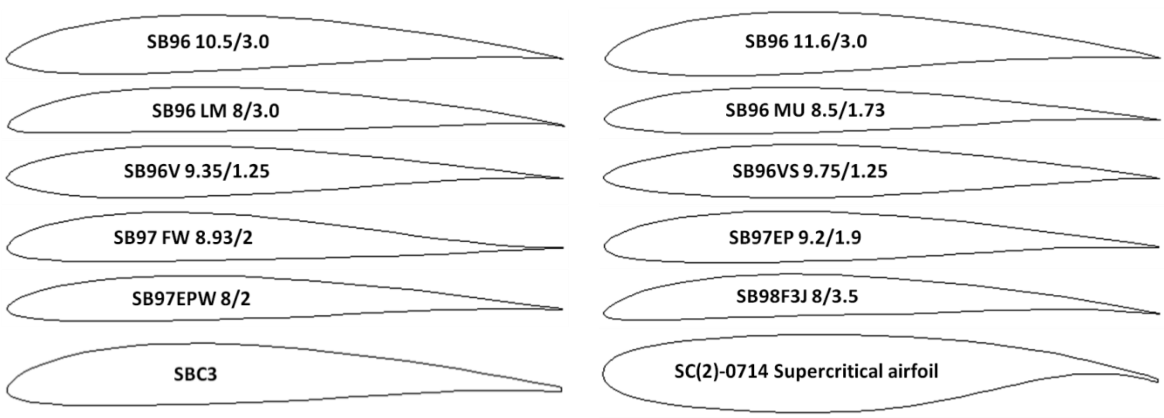

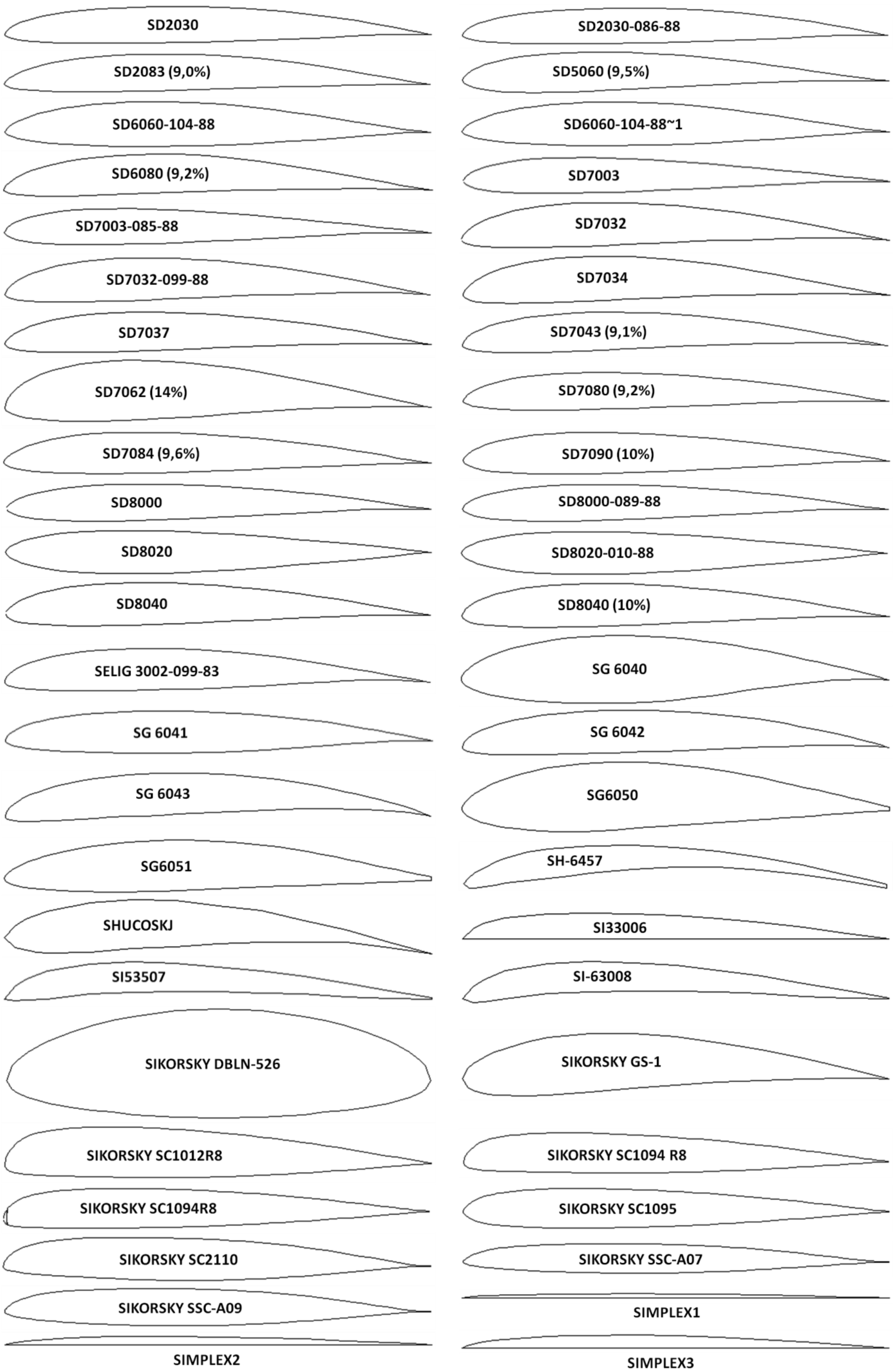

SD2030
SD2030-086-88
SD2083 (9,0%)
SD5060 (9,5%)
SD6060-104-88
SD6060-104-88~1
SD6080 (9,2%)
SD7003
SD7003-085-88
SD7032
SD7032-099-88
SD7034
SD7037
SD7043 (9,1%)
SD7062 (14%)
SD7080 (9,2%)
SD7084 (9,6%)
SD7090 (10%)
SD8000
SD8000-089-88
SD8020
SD8020-010-88
SD8040
SD8040 (10%)
SELIG 3002-099-83
SG 6040
SG 6041
SG 6042
SG 6043
SG6050
SG6051
SH-6457
SHUCOSKJ
SI33006
SI53507
SI-63008
SIKORSKY DBLN-526
SIKORSKY GS-1
SIKORSKY SC1012R8
SIKORSKY SC1094 R8
SIKORSKY SC1094R8
SIKORSKY SC1095
SIKORSKY SC2110
SIKORSKY SSC-A07
SIKORSKY SSC-A09
SIMPLEX1
SIMPLEX2
SIMPLEX3

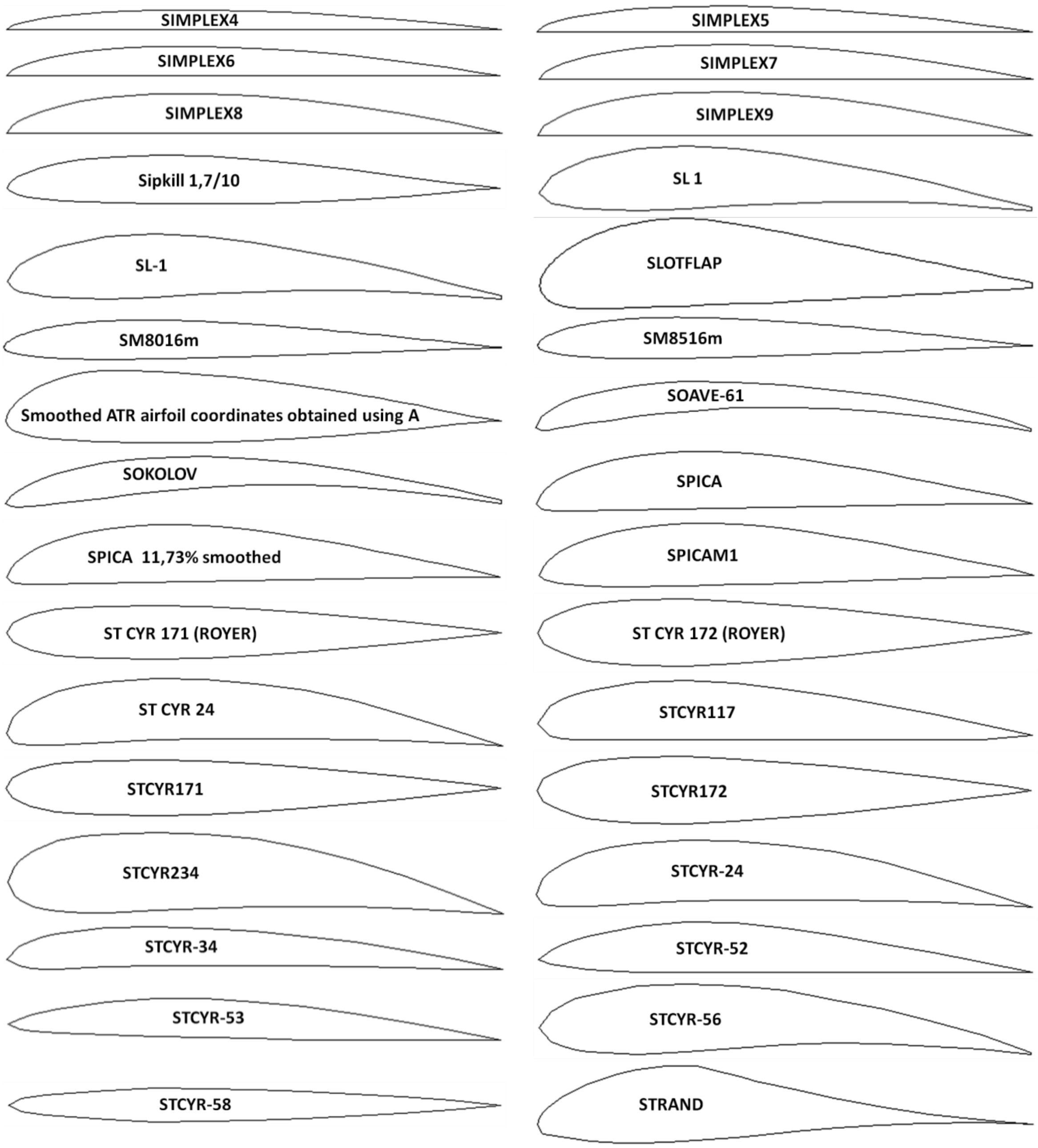

Results and discussion

The calculated pressure contours on the surfaces of the airfoils at different angles of attack are presented in the Figs. 1-92. The calculated values on the scale can be represented as the basic values when comparing the pressure drop under conditions of changing the angle of attack of the airfoils.

92 airfoils of the SB, SD, SIKORSKY, SIMPLEX, ST CYR and others types were considered in this paper. All airfoils are asymmetrical, with the exception of SD8020, SD 8020-010-88, ST CYR 171 (ROYER), ST CYR 172 (ROYER) and STCYR-58. The largest and smallest thicknesses of the studied airfoils are 25.99% and 0.99% for SIKORSKY DBLN-526 and SIMPLEX1, respectively. The largest and smallest cambers are 8.6% and 0.0% for STCYR234 and all symmetrical airfoils, respectively. The largest and smallest leading edge radii are 3.2415% and 0.4056% for STCYR234 and SIKORSKY SSC-A07, respectively. The largest and smallest trailing edge thicknesses are 1.0% and 0.0% for SG6050, SG6051 and SBC3 and for the most airfoils, respectively.

Let us consider in detail the aerodynamic characteristics of some airfoils: SC(2)-0714 Supercritical airfoil, SD7062 (14%), SG 6040, SI-63008, SIKORSKY DBLN-526, SIMPLEX1 and STCYR-58.

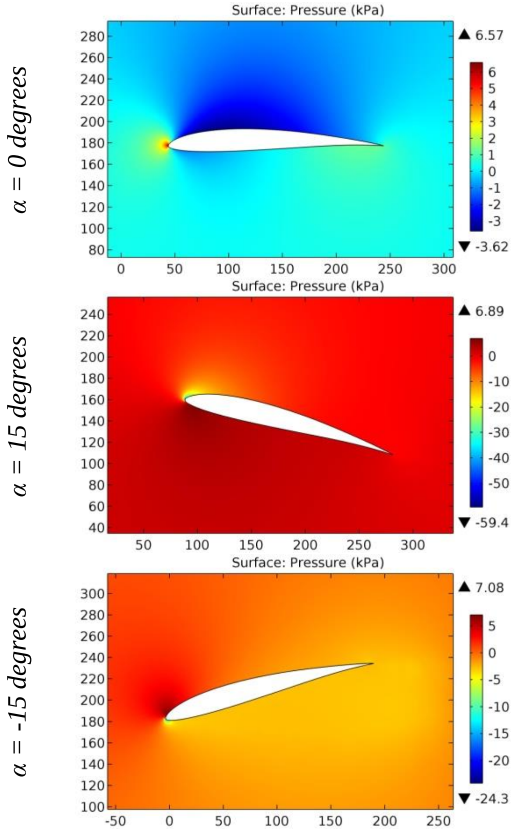

Figure 1. The pressure contours on the surfaces of the SB96 10.5/3.0 airfoil.

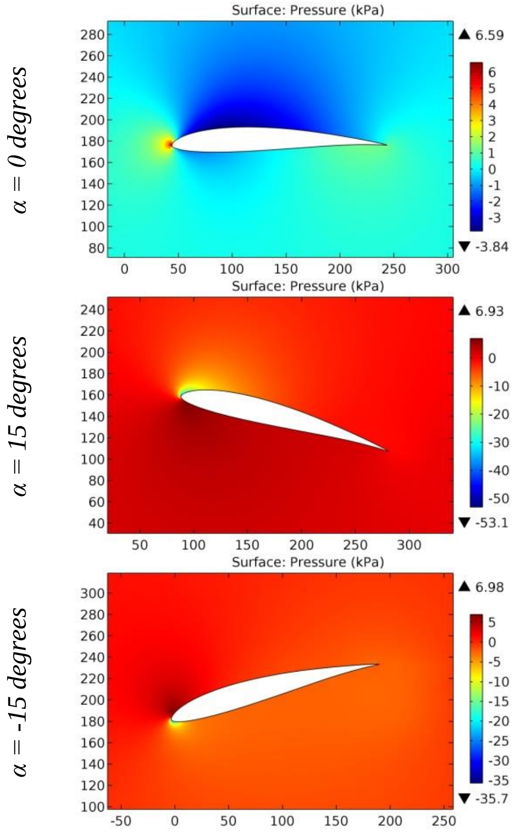

Figure 2. The pressure contours on the surfaces of the SB96 11.6/3.0 airfoil.

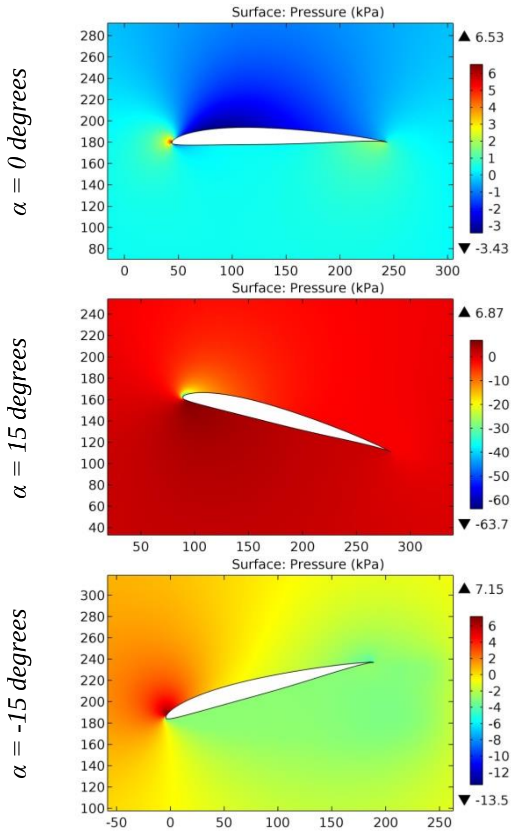

Figure 3. The pressure contours on the surfaces of the SB96 LM 8/3.0 airfoil.

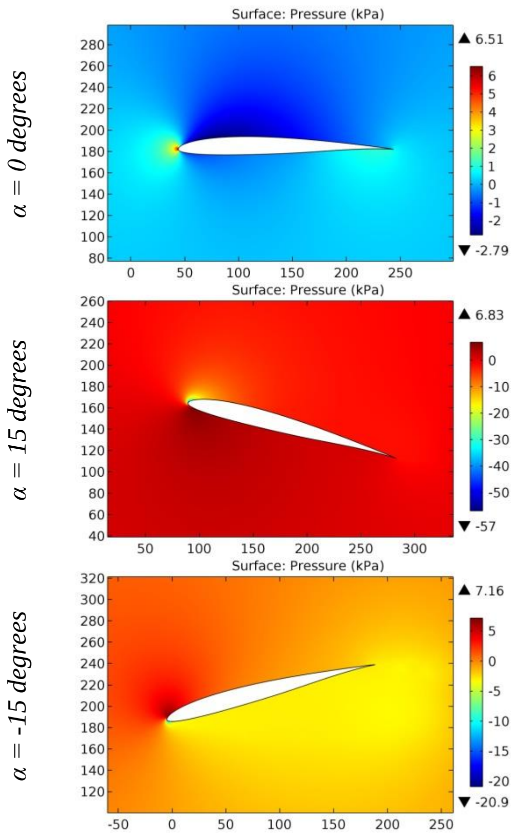

Figure 4. The pressure contours on the surfaces of the SB96 MU 8.5/1.73 airfoil.

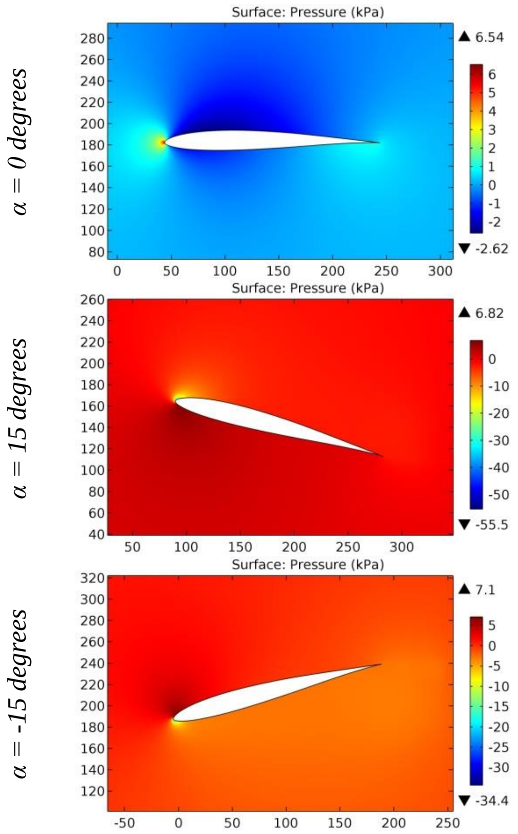

Figure 5. The pressure contours on the surfaces of the SB96V 9.35/1.25 airfoil.

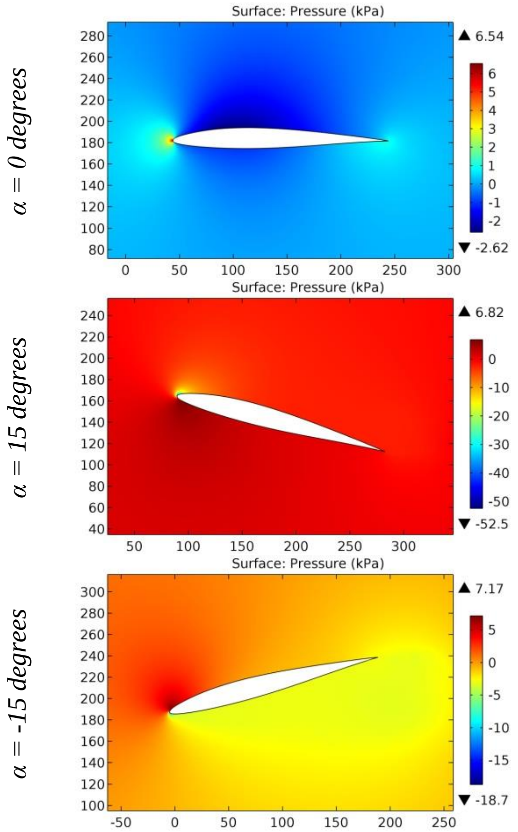

Figure 6. The pressure contours on the surfaces of the SB96VS 9.75/1.25 airfoil.

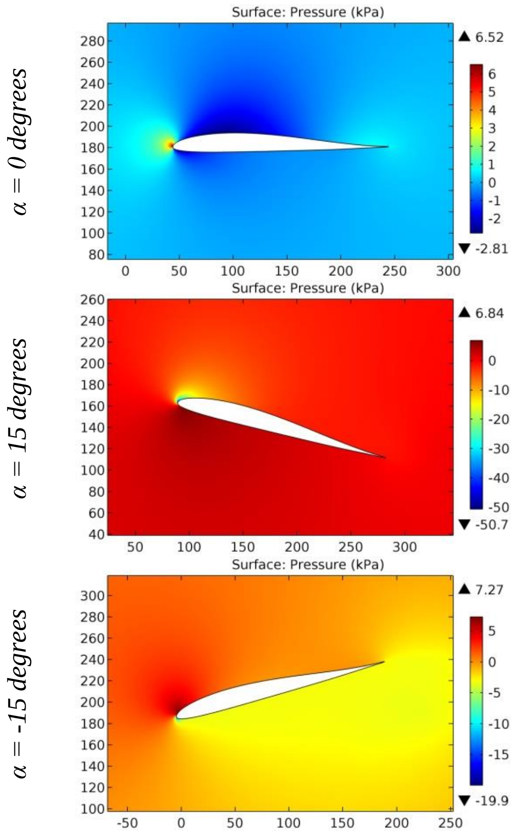

Figure 7. The pressure contours on the surfaces of the SB97 FW 8.93/2 airfoil.

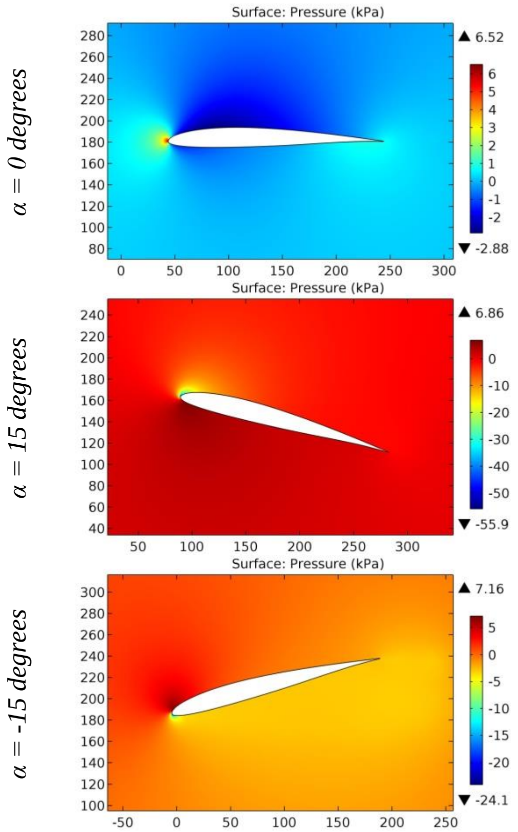

Figure 8. The pressure contours on the surfaces of the SB97EP 9.2/1.9 airfoil.

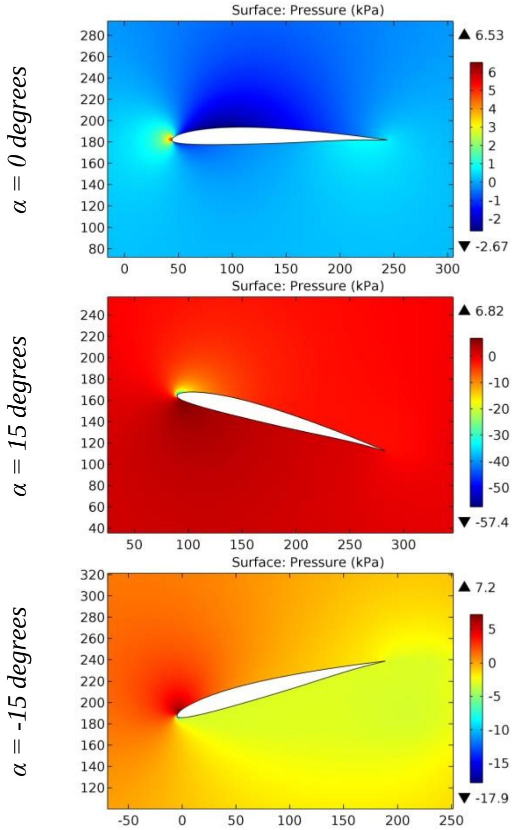

Figure 9. The pressure contours on the surfaces of the SB97EPW 8/2 airfoil.

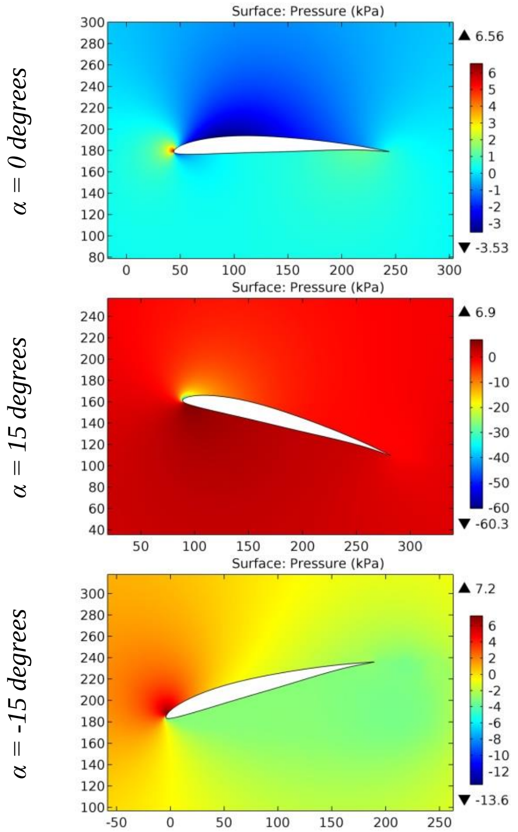

Figure 10. The pressure contours on the surfaces of the SB98F3J 8/3.5 airfoil.

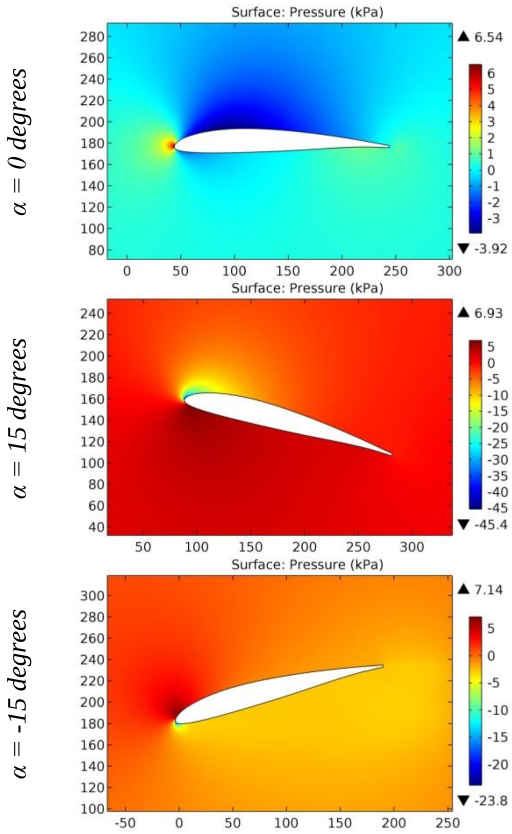

Figure 11. The pressure contours on the surfaces of the SBC3 airfoil.

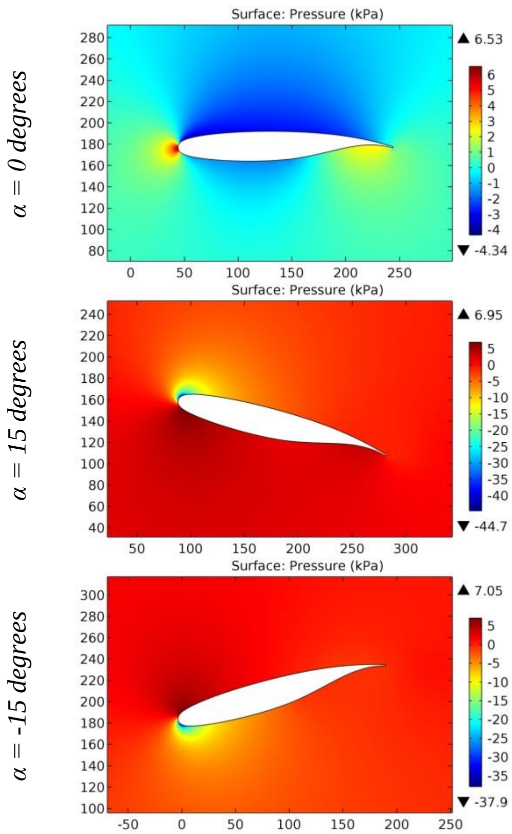

Figure 12. The pressure contours on the surfaces of the SC(2)-0714 Supercritical airfoil.

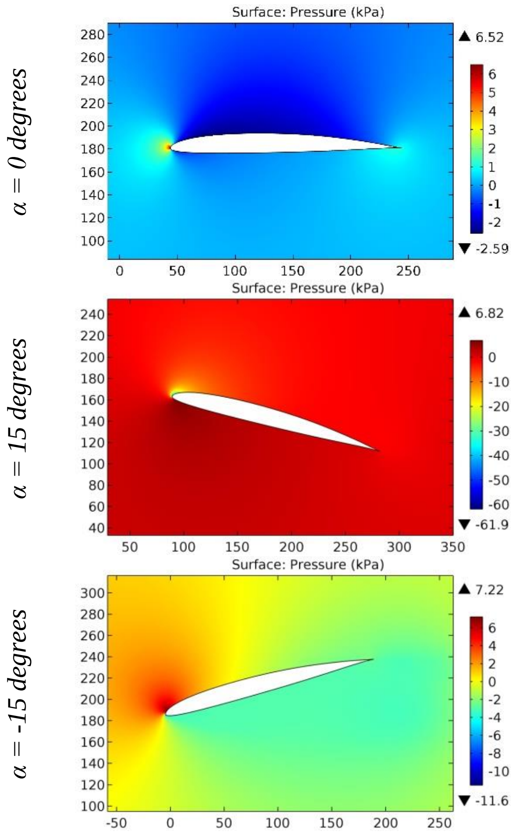

Figure 13. The pressure contours on the surfaces of the SD2030 airfoil.

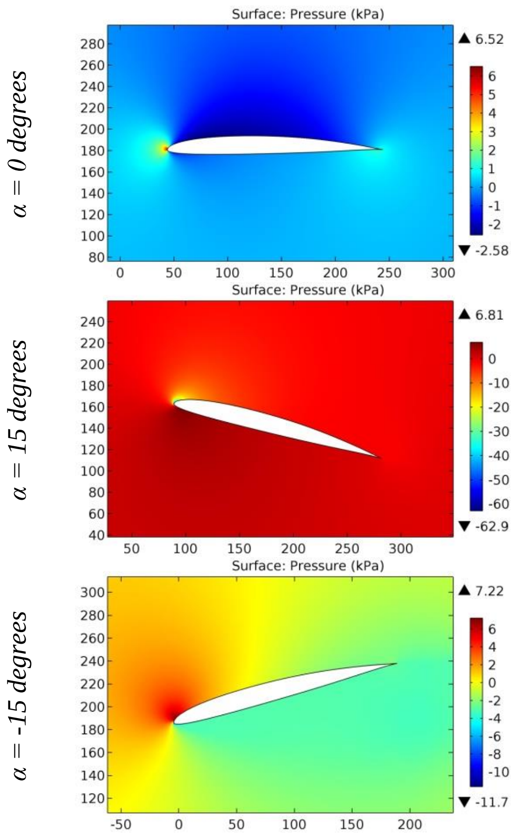

Figure 14. The pressure contours on the surfaces of the SD2030-086-88 airfoil.

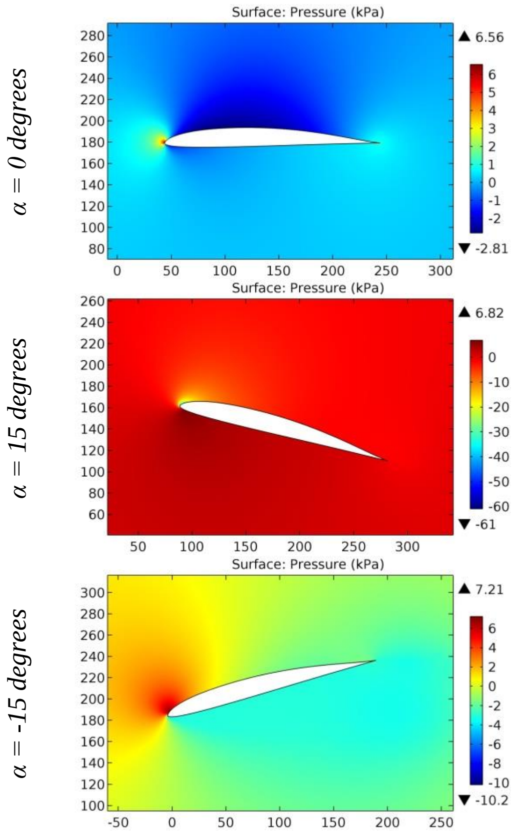

Figure 15. The pressure contours on the surfaces of the SD2083 (9,0%) airfoil.

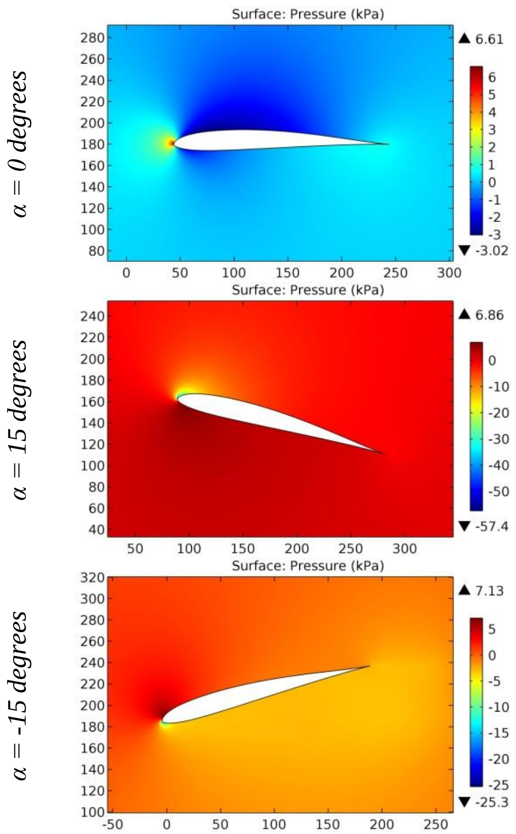

Figure 16. The pressure contours on the surfaces of the SD5060 (9,5%) airfoil.

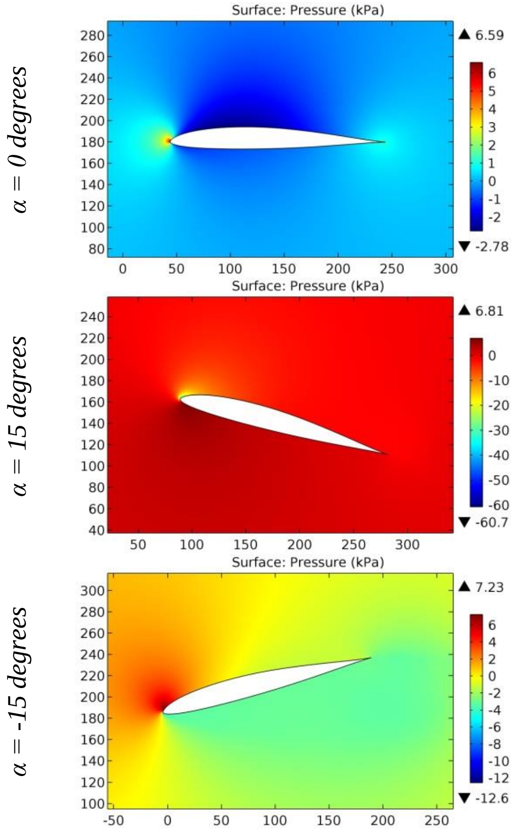

Figure 17. The pressure contours on the surfaces of the SD6060-104-88 airfoil.

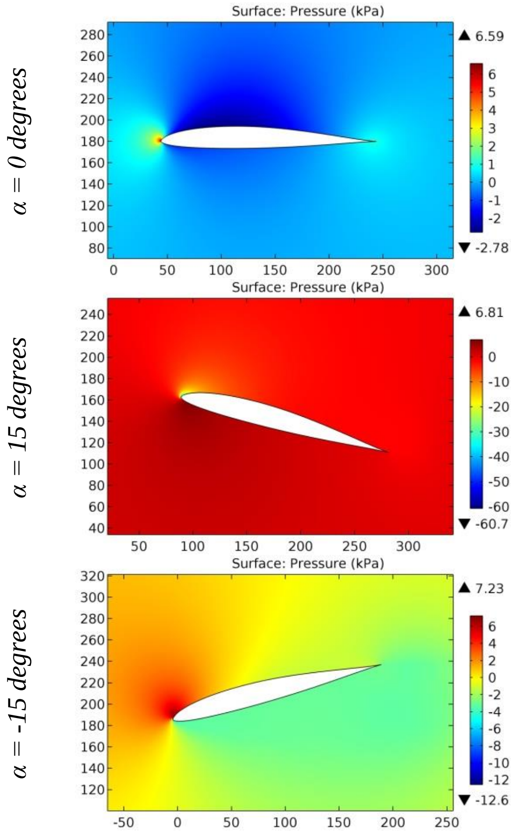

Figure 18. The pressure contours on the surfaces of the SD6060-104-88~1 airfoil.

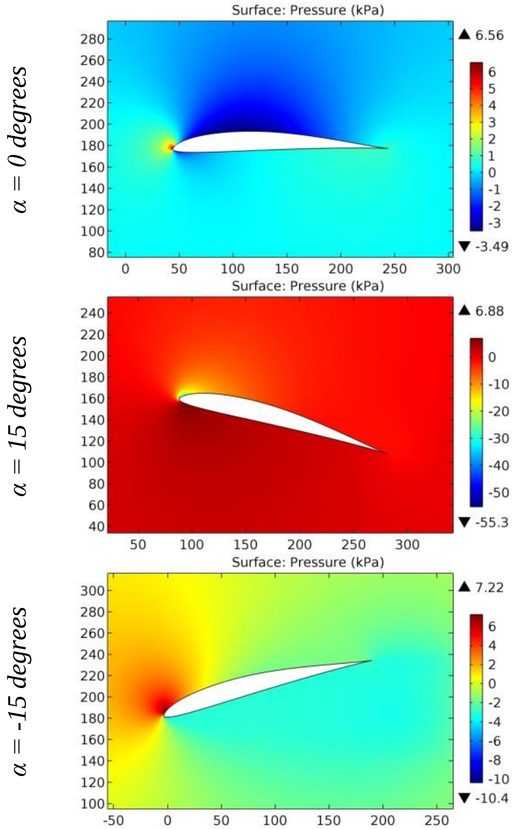

Figure 19. The pressure contours on the surfaces of the SD6080 (9,2%) airfoil.

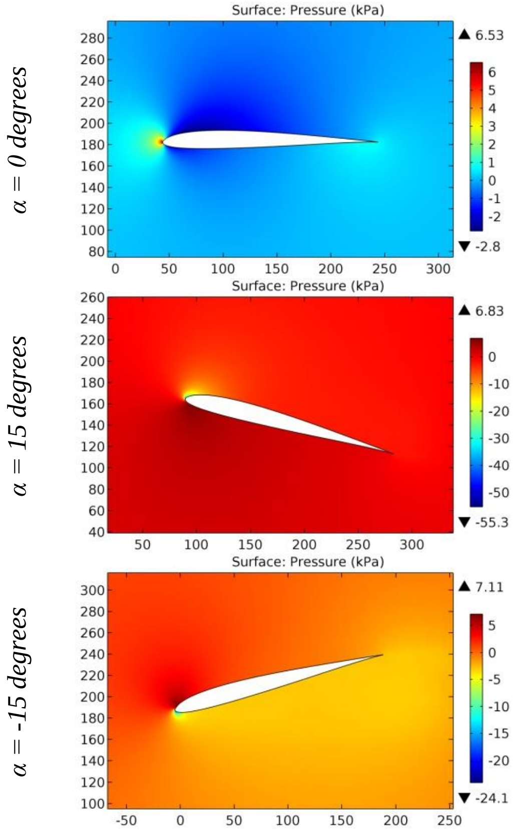

Figure 20. The pressure contours on the surfaces of the SD7003 airfoil.

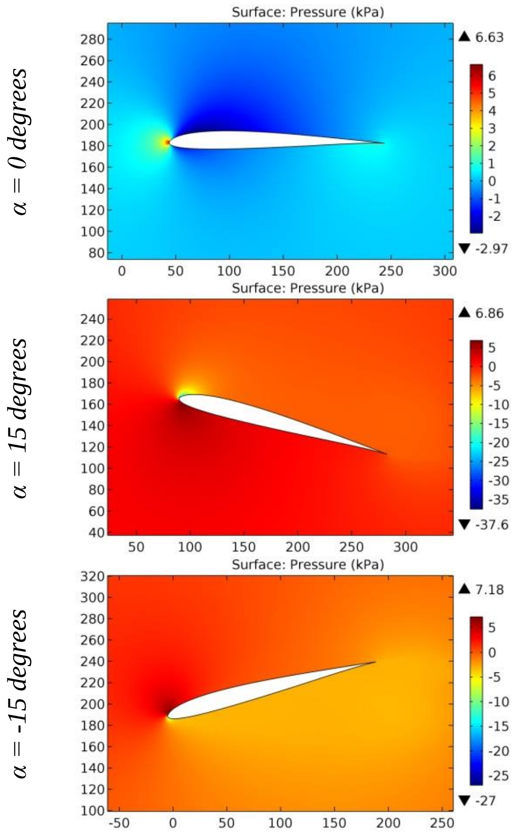

Figure 21. The pressure contours on the surfaces of the SD7003-085-88 airfoil.

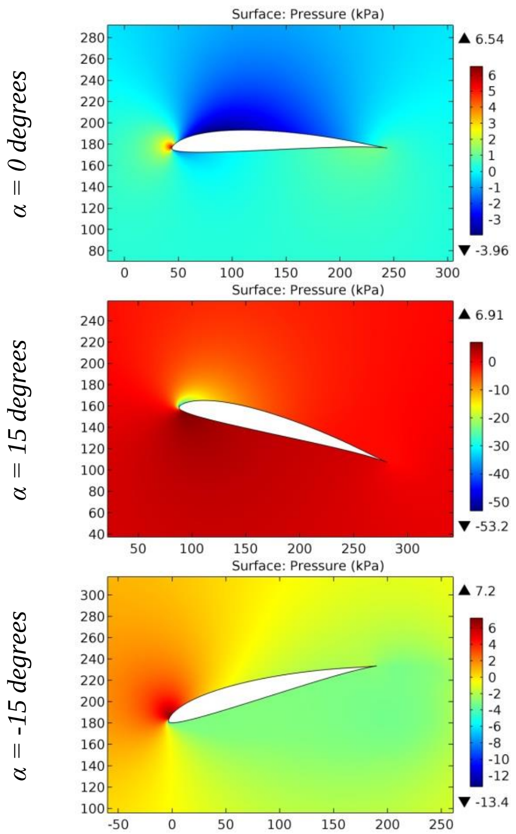

Figure 22. The pressure contours on the surfaces of the SD7032 airfoil.

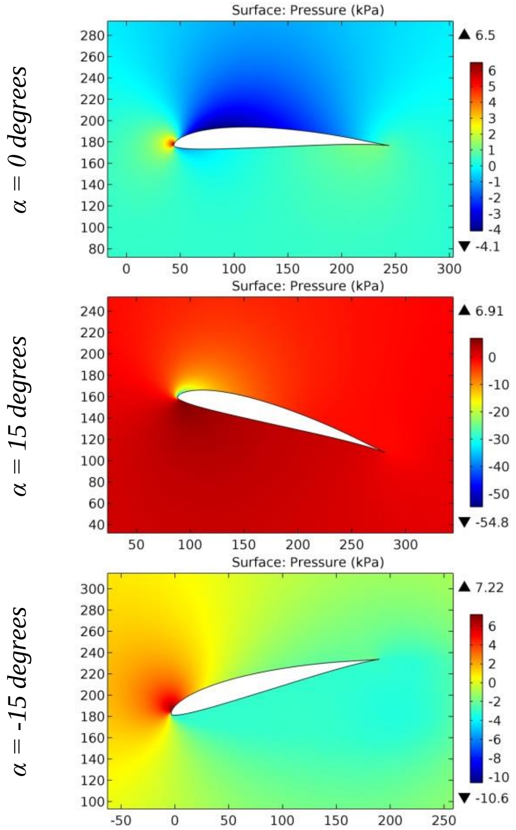

Figure 23. The pressure contours on the surfaces of the SD7032-099-88 airfoil.

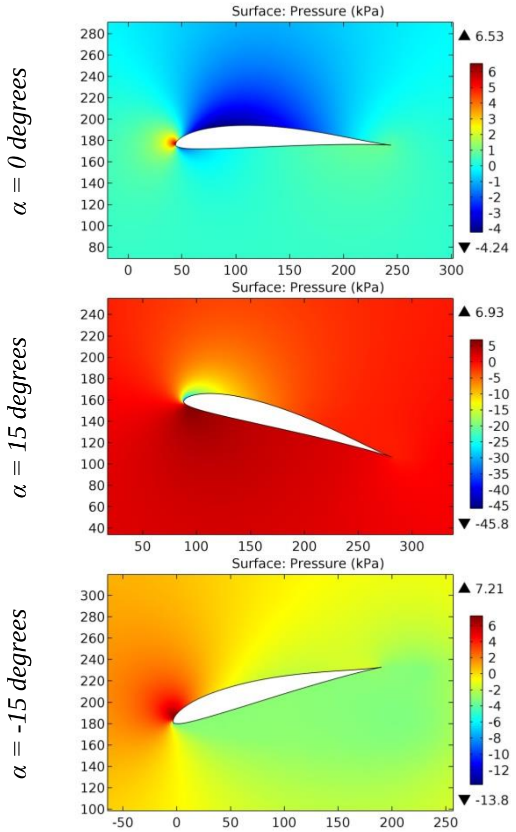

Figure 24. The pressure contours on the surfaces of the SD7034 airfoil.

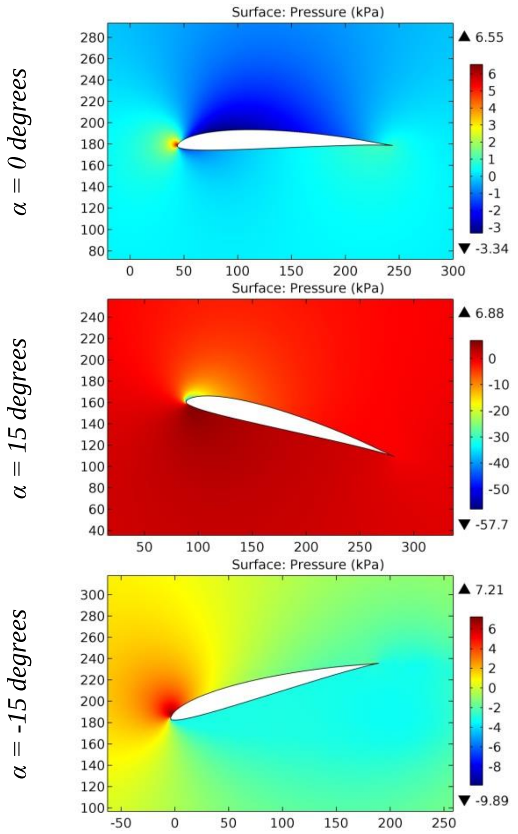

Figure 25. The pressure contours on the surfaces of the SD7037 airfoil.

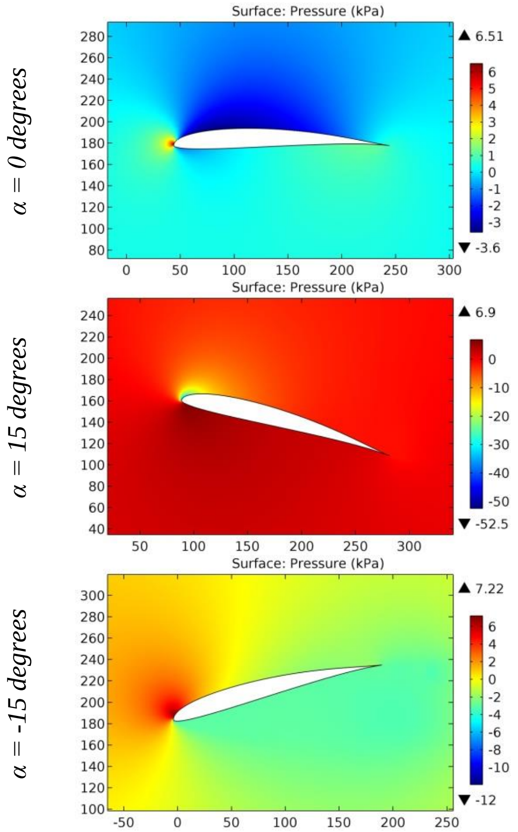

Figure 26. The pressure contours on the surfaces of the SD7043 (9,1%) airfoil.

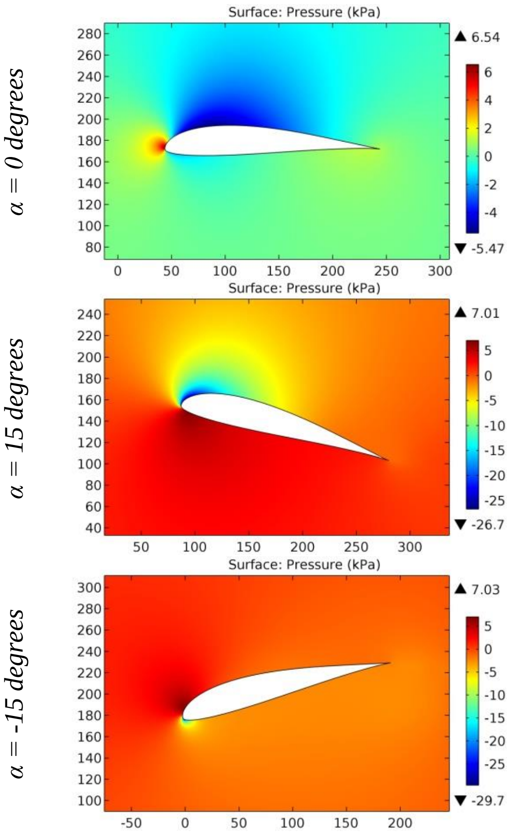

Figure 27. The pressure contours on the surfaces of the SD7062 (14%) airfoil.

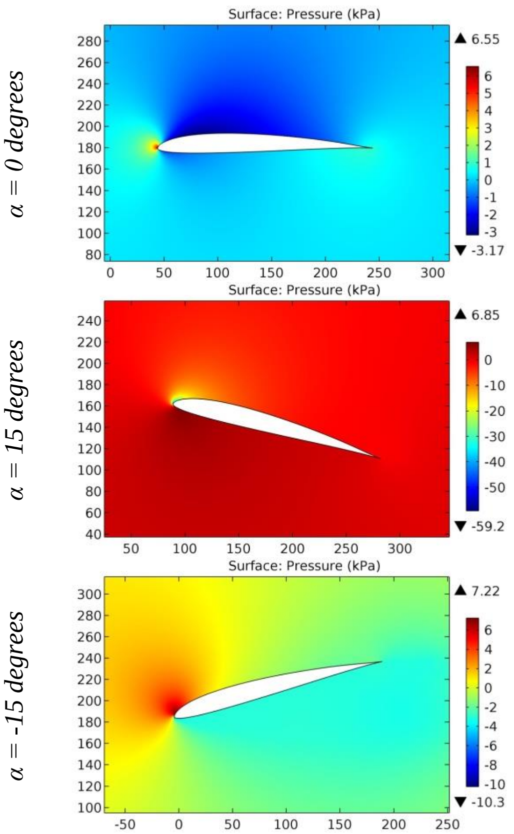

Figure 28. The pressure contours on the surfaces of the SD7080 (9,2%) airfoil.

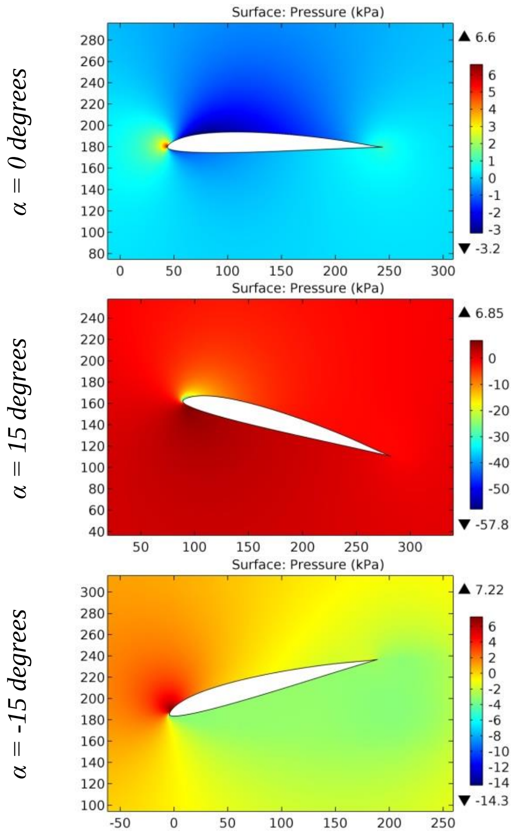

Figure 29. The pressure contours on the surfaces of the SD7084 (9,6%) airfoil.

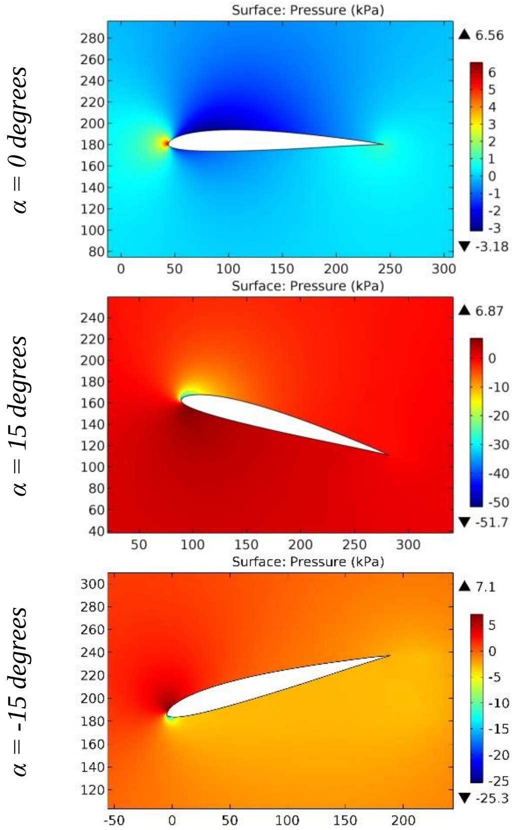

Figure 30. The pressure contours on the surfaces of the SD7090 (10%) airfoil.

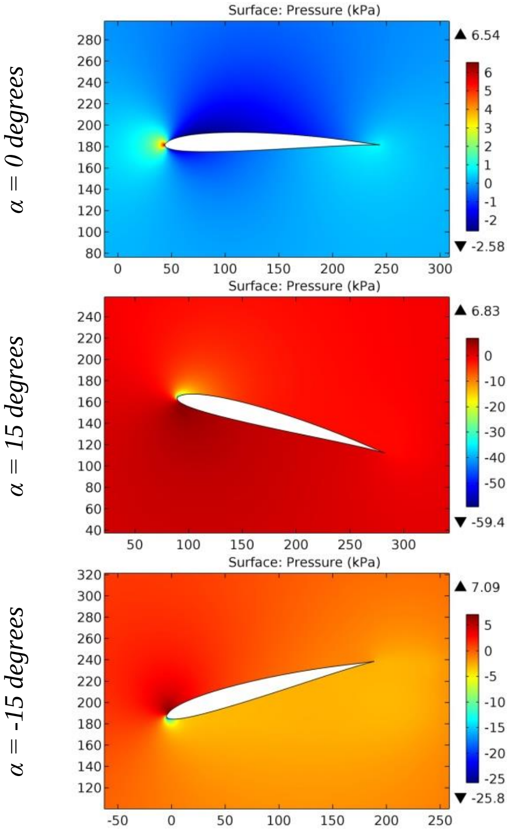

Figure 31. The pressure contours on the surfaces of the SD8000 airfoil.

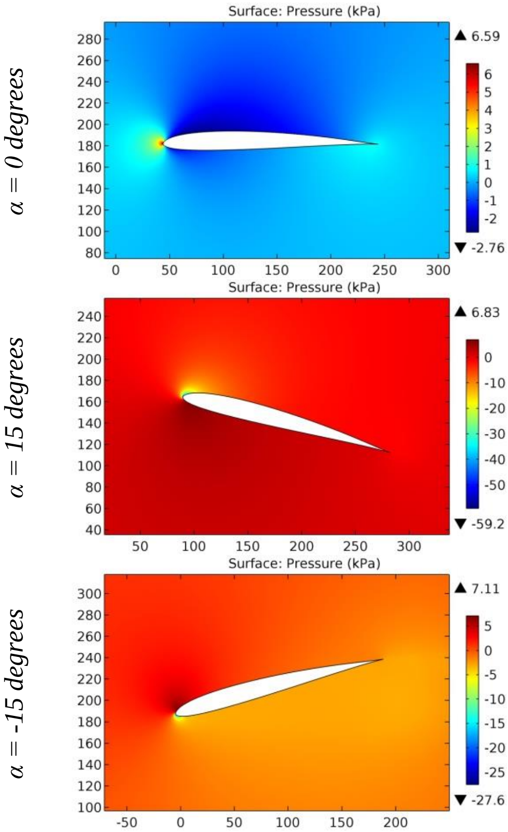

Figure 32. The pressure contours on the surfaces of the SD8000-089-88 airfoil.

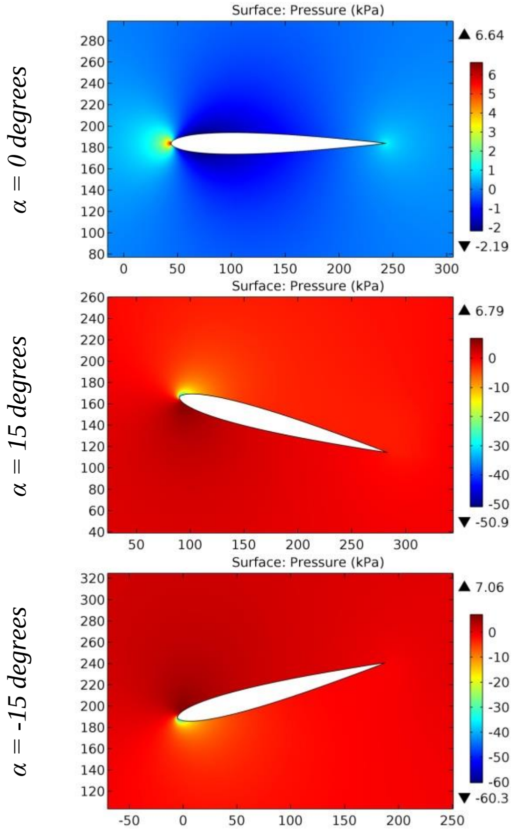

Figure 33. The pressure contours on the surfaces of the SD8020 airfoil.

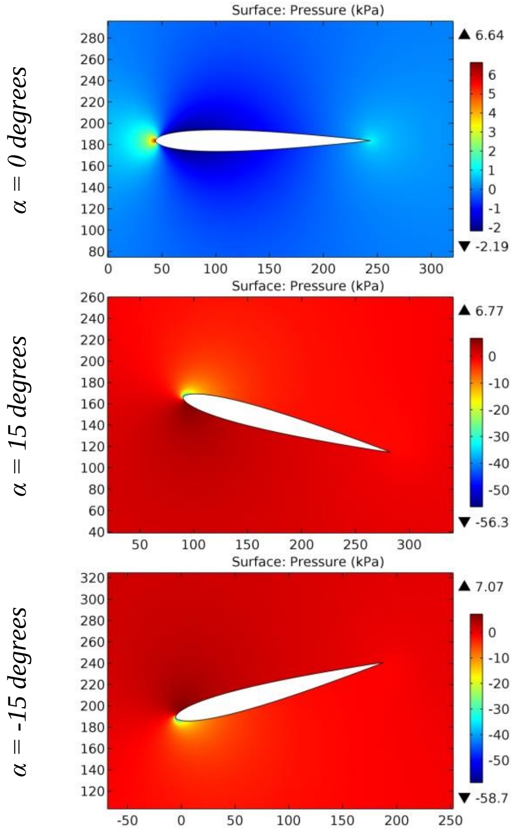

Figure 34. The pressure contours on the surfaces of the SD8020-010-88 airfoil.

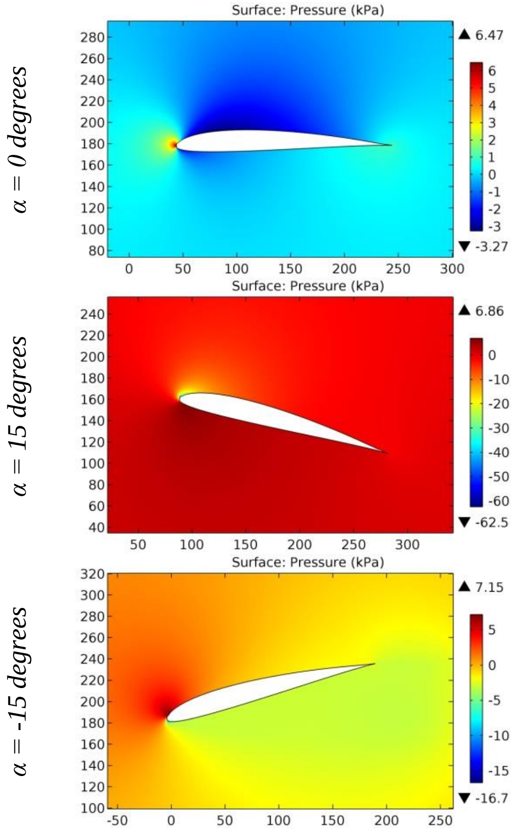

Figure 35. The pressure contours on the surfaces of the SD8040 airfoil.

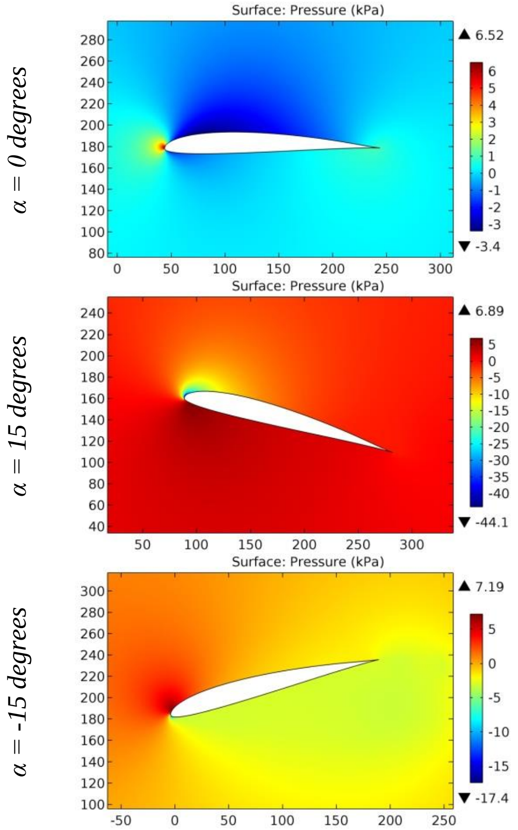

Figure 36. The pressure contours on the surfaces of the SD8040 (10%) airfoil.

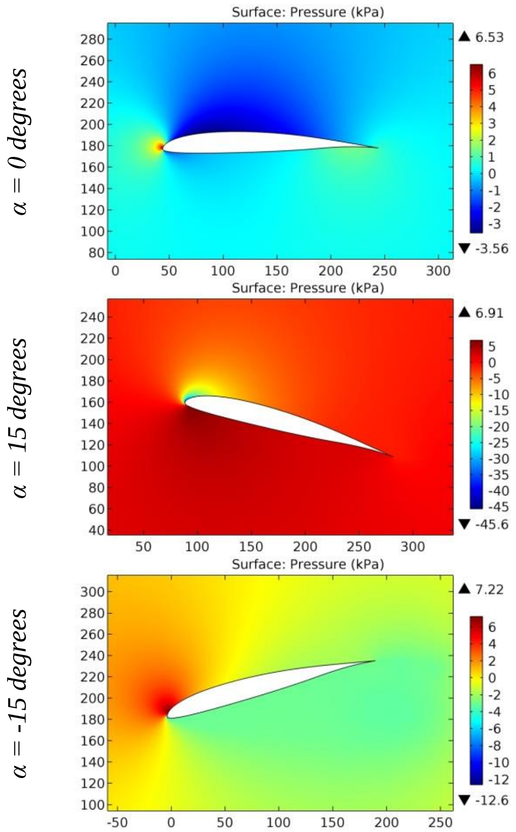

Figure 37. The pressure contours on the surfaces of the SELIG 3002-099-83 airfoil.

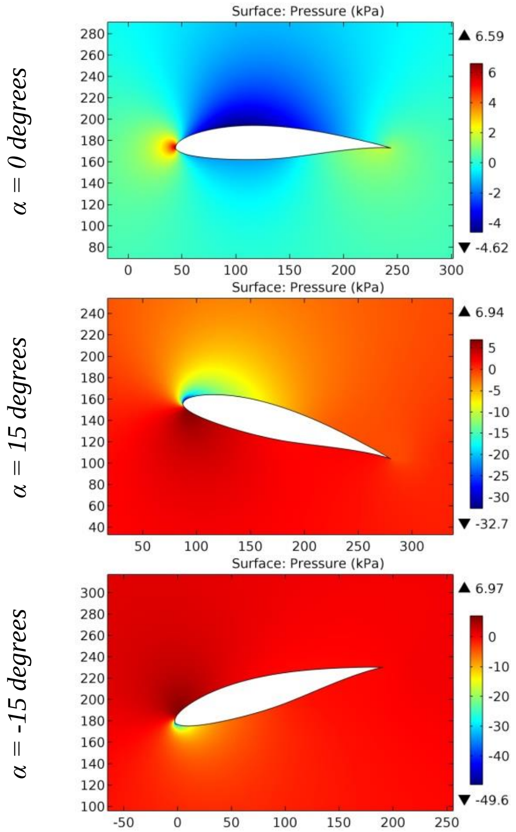

Figure 38. The pressure contours on the surfaces of the SG 6040 airfoil.

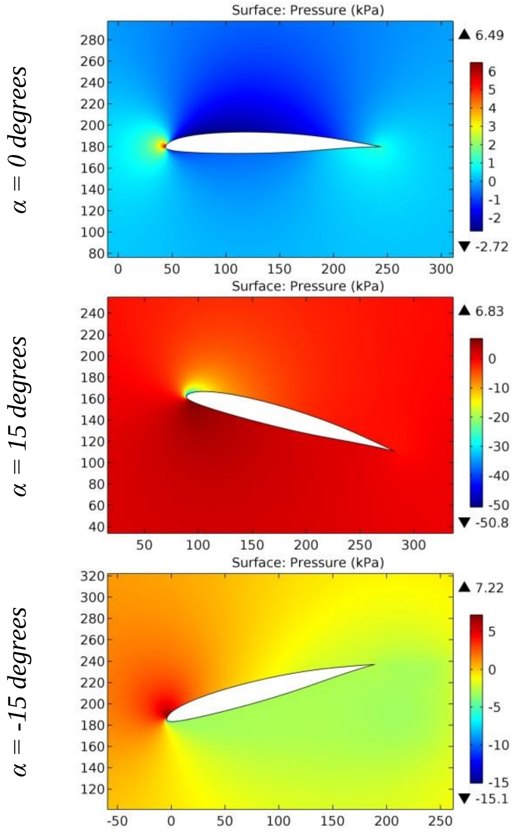

Figure 39. The pressure contours on the surfaces of the SG 6041 airfoil.

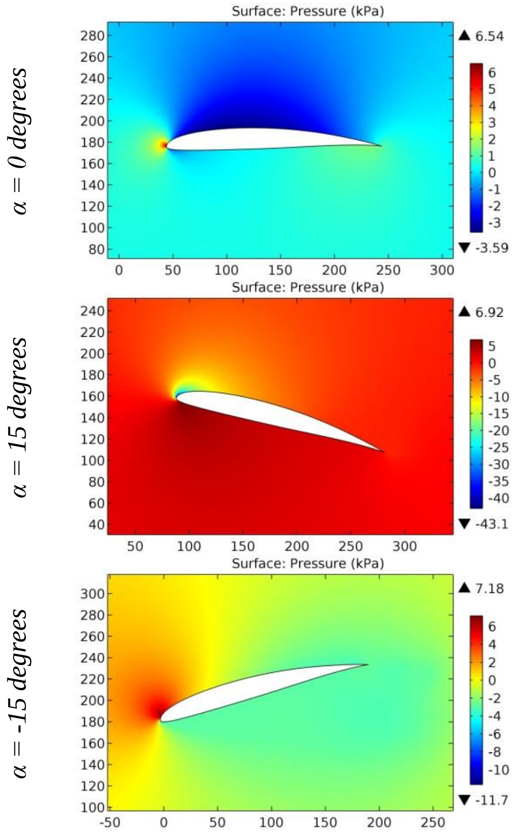

Figure 40. The pressure contours on the surfaces of the SG 6042 airfoil.

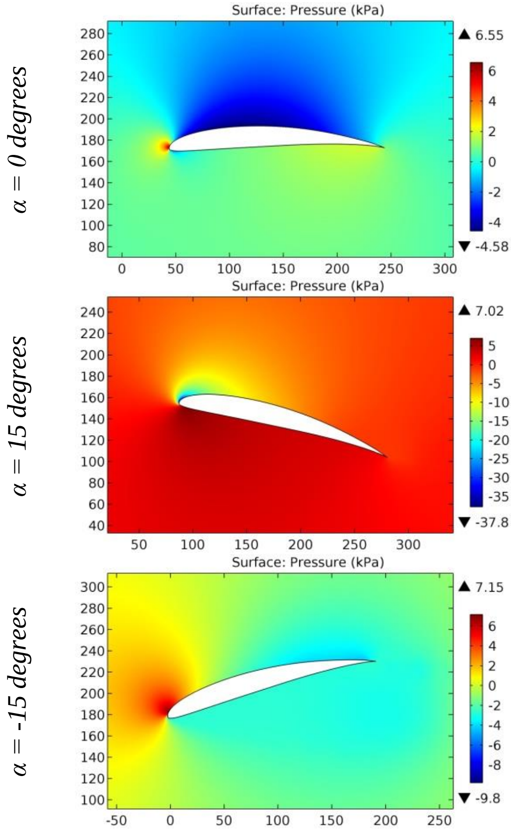

Figure 41. The pressure contours on the surfaces of the SG 6043 airfoil.

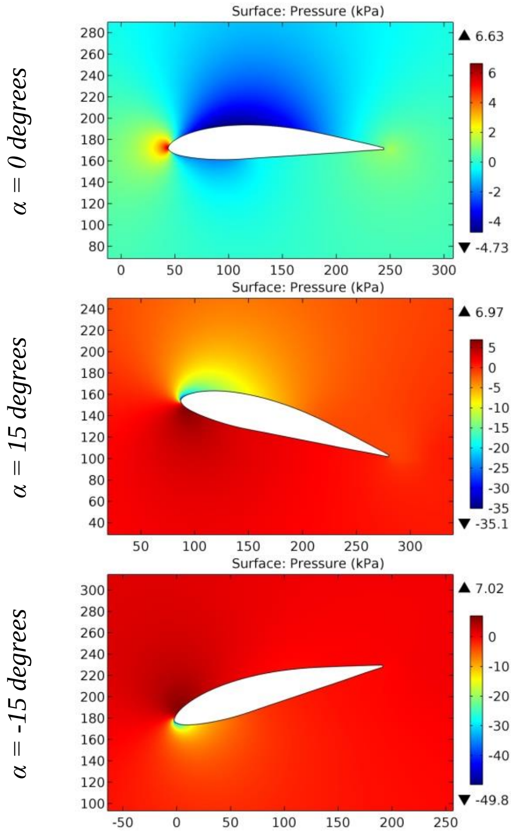

Figure 42. The pressure contours on the surfaces of the SG6050 airfoil.

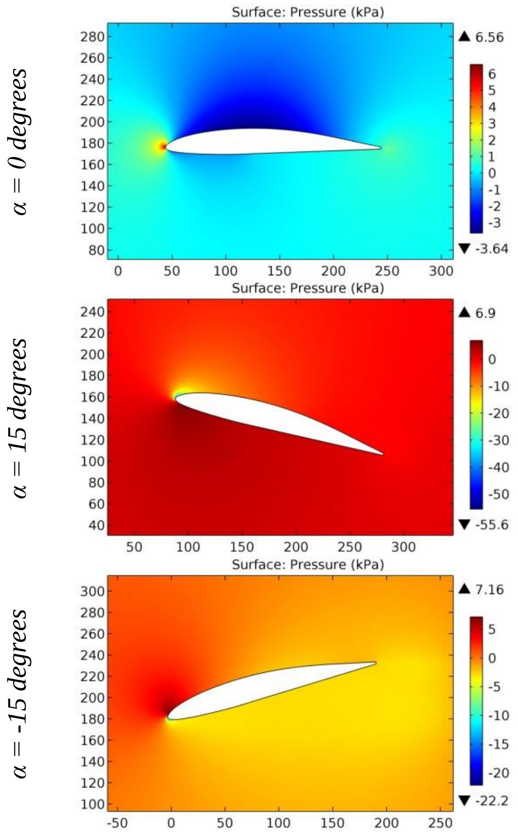

Figure 43. The pressure contours on the surfaces of the SG6051 airfoil.

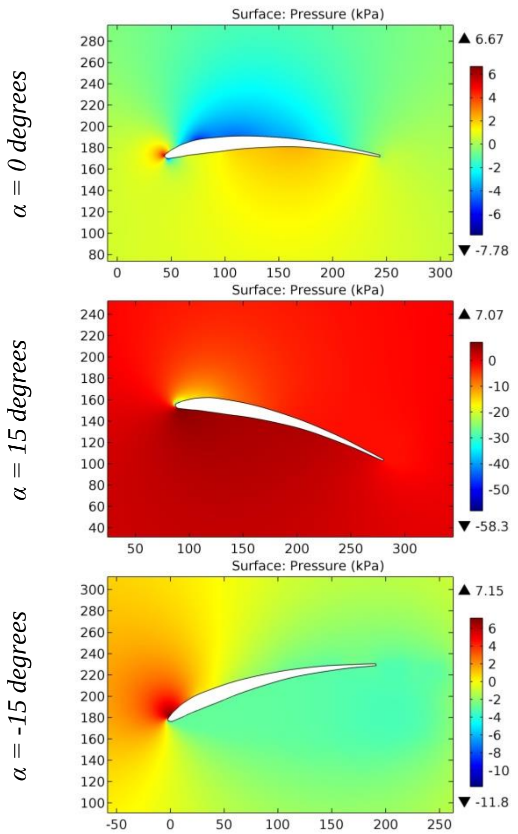

Figure 44. The pressure contours on the surfaces of the SH-6457 airfoil.

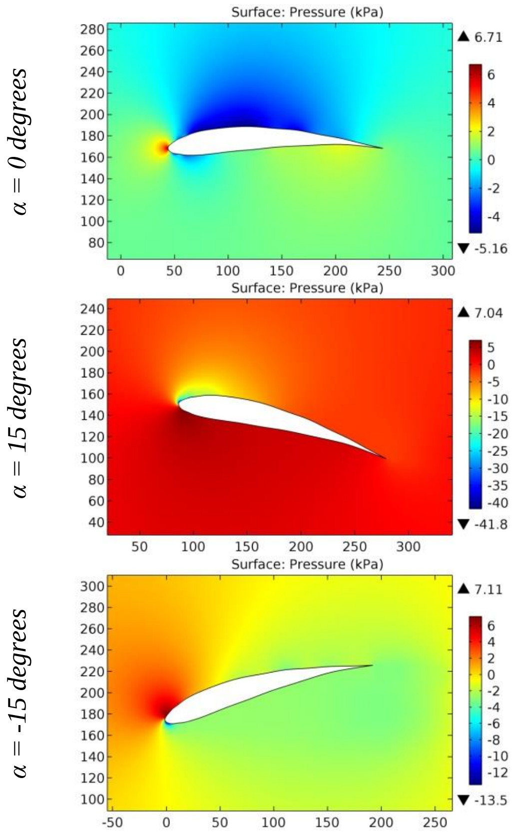

Figure 45. The pressure contours on the surfaces of the SHUCOSKJ airfoil.

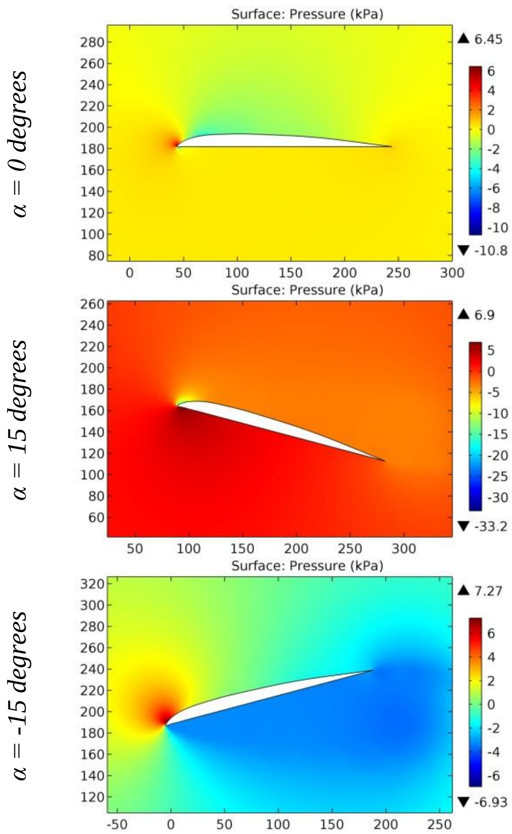

Figure 46. The pressure contours on the surfaces of the SI33006 airfoil.

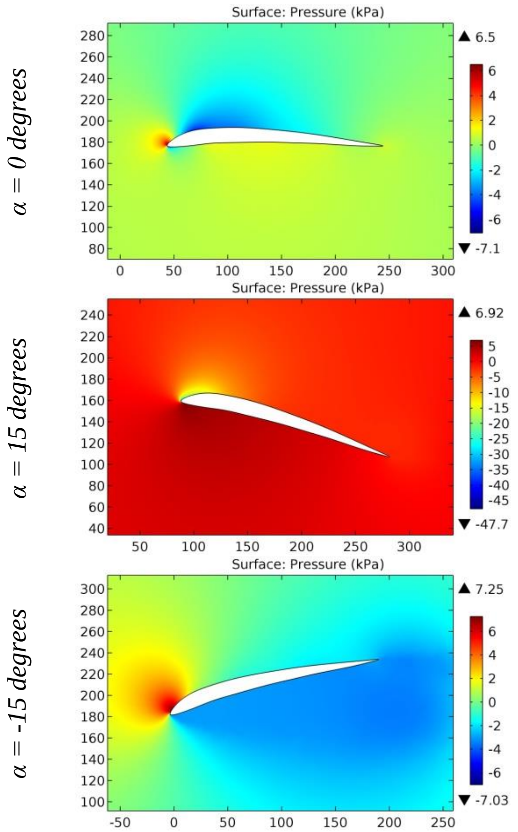

Figure 47. The pressure contours on the surfaces of the SI53507 airfoil.

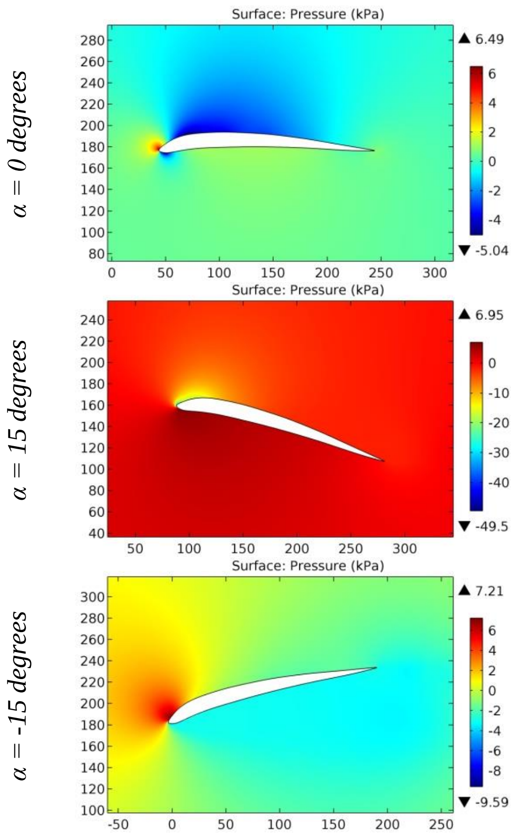

Figure 48. The pressure contours on the surfaces of the SI-63008 airfoil.

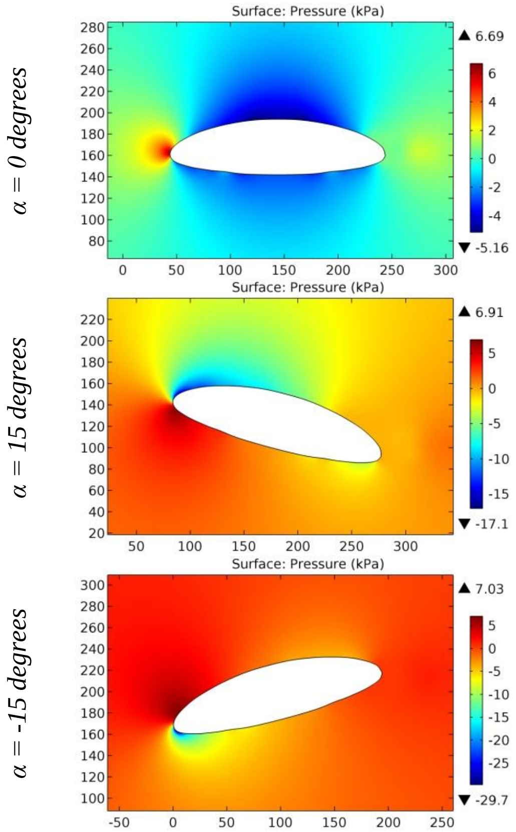

Figure 49. The pressure contours on the surfaces of the SIKORSKY DBLN-526 airfoil.

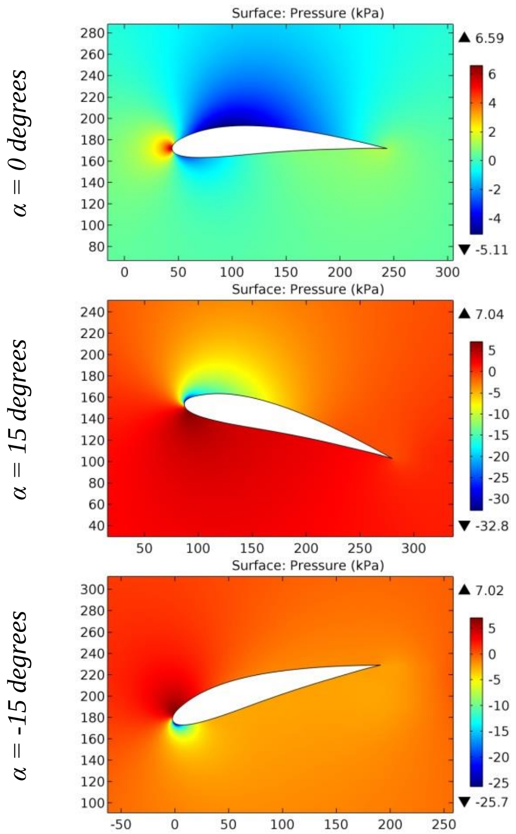

Figure 50. The pressure contours on the surfaces of the SIKORSKY GS-1 airfoil.

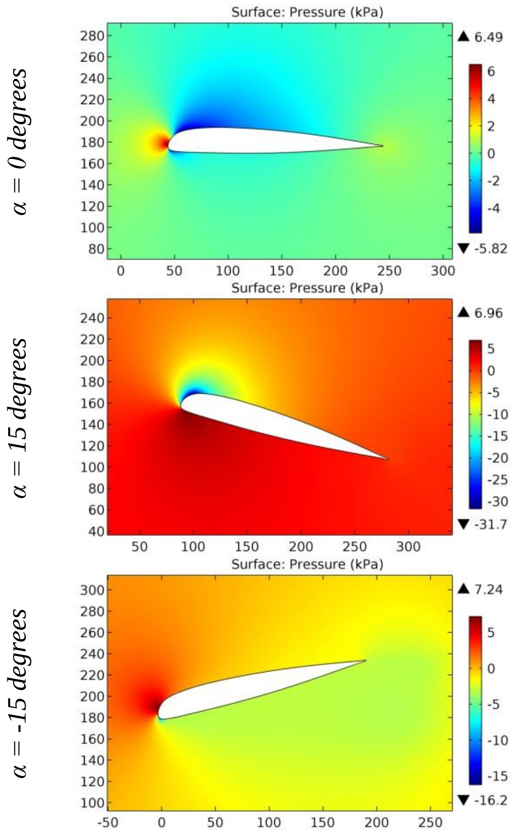

Figure 51. The pressure contours on the surfaces of the SIKORSKY SC1012R8 airfoil.

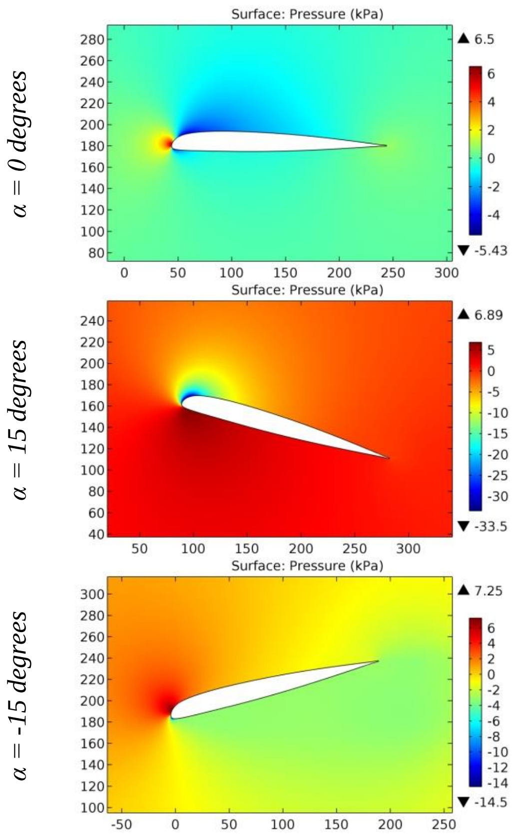

Figure 52. The pressure contours on the surfaces of the SIKORSKY SC1094 R8 airfoil.

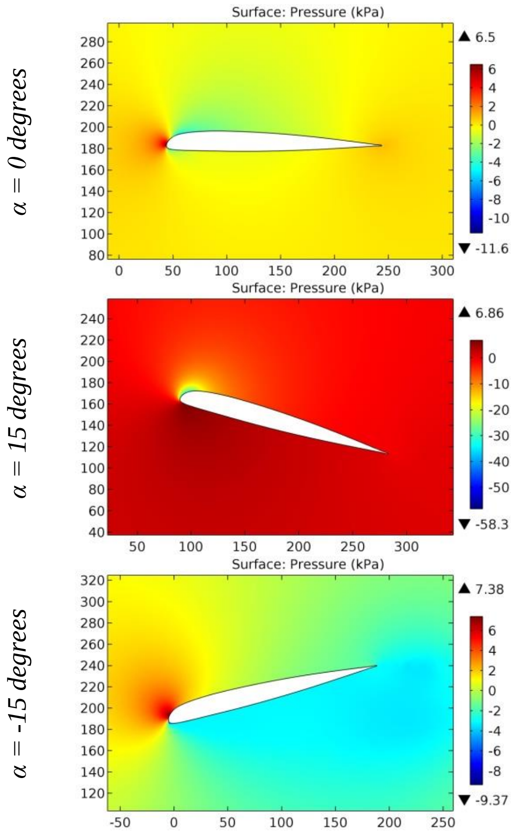

Figure 53. The pressure contours on the surfaces of the SIKORSKY SC1094R8 airfoil.

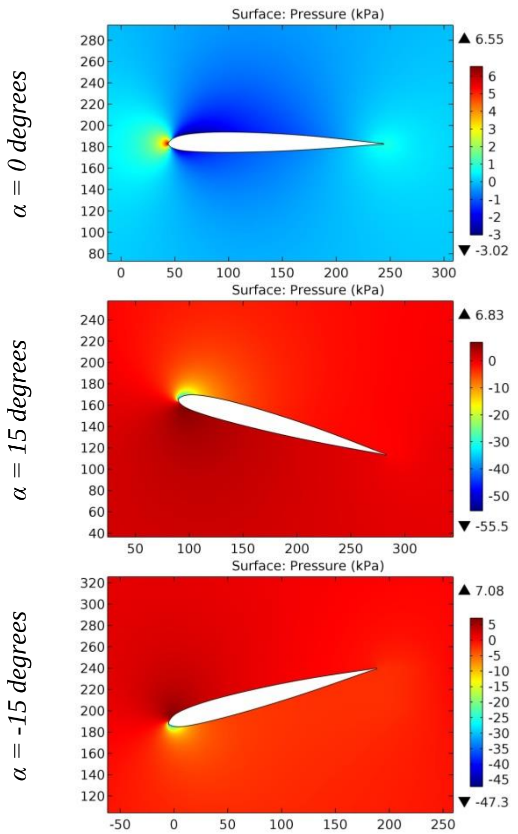

Figure 54. The pressure contours on the surfaces of the SIKORSKY SC1095 airfoil.

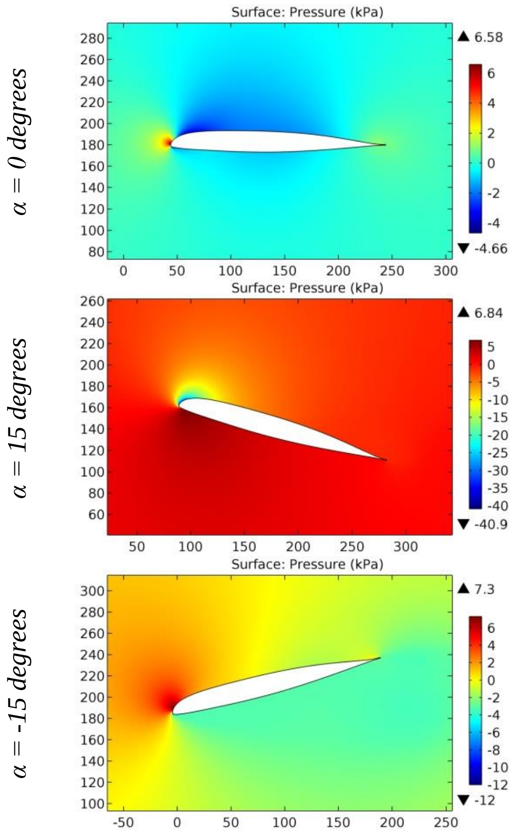

Figure 55. The pressure contours on the surfaces of the SIKORSKY SC2110 airfoil.

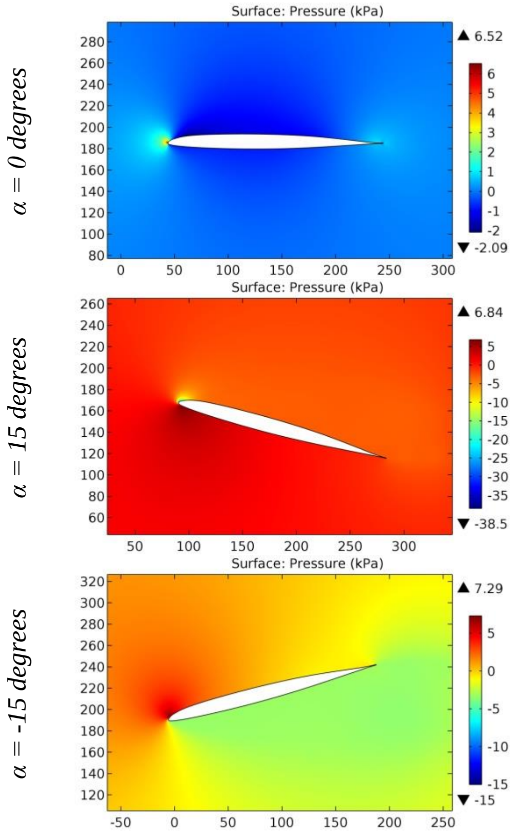

Figure 56. The pressure contours on the surfaces of the SIKORSKY SSC-A07 airfoil.

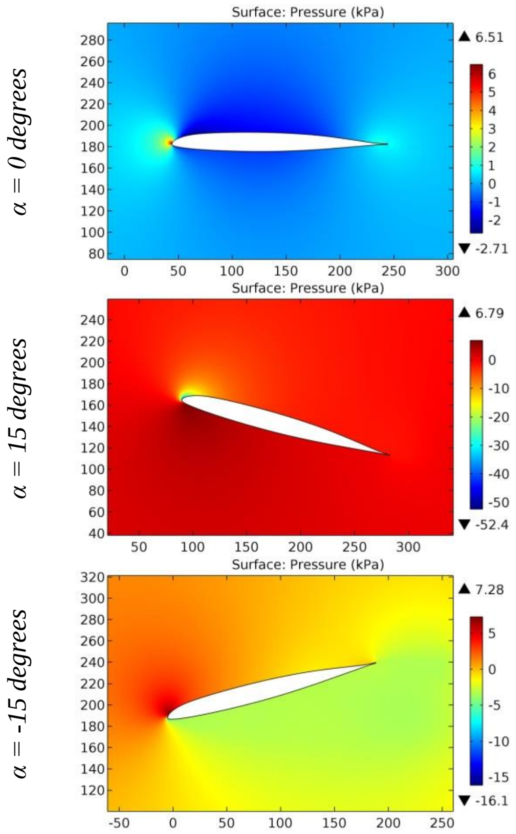

Figure 57. The pressure contours on the surfaces of the SIKORSKY SSC-A09 airfoil.

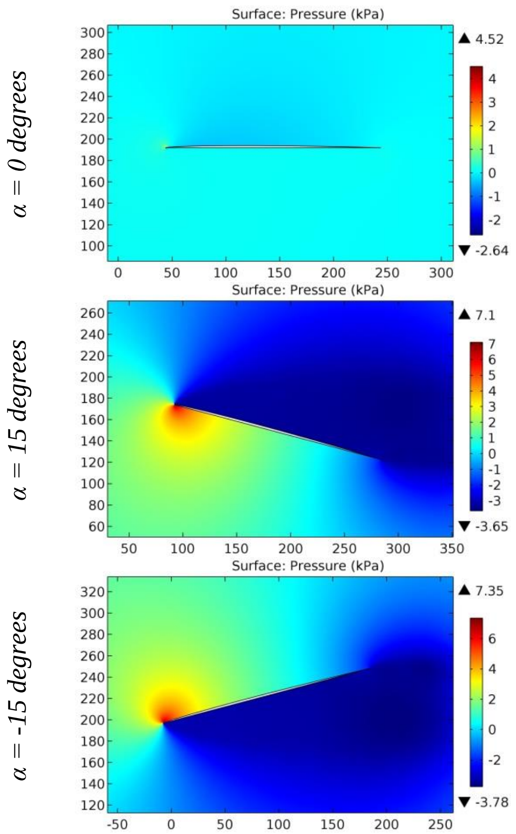

Figure 58. The pressure contours on the surfaces of the SIMPLEX1 airfoil.

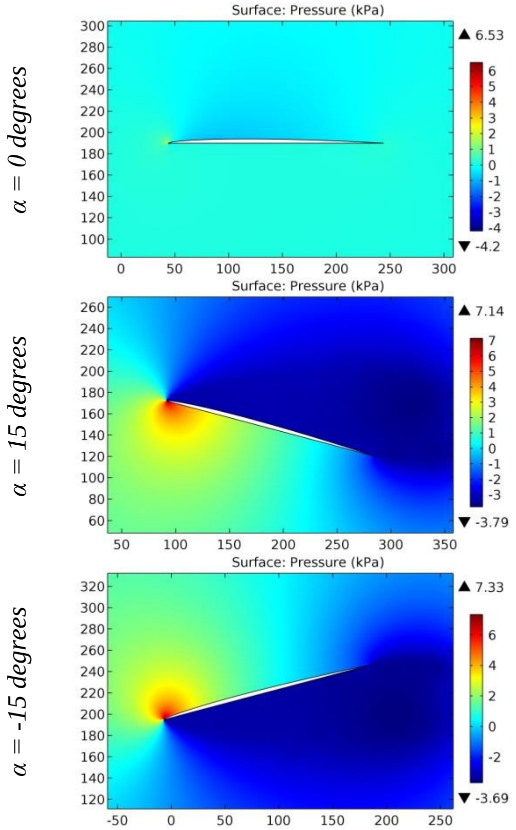

Figure 59. The pressure contours on the surfaces of the SIMPLEX2 airfoil.

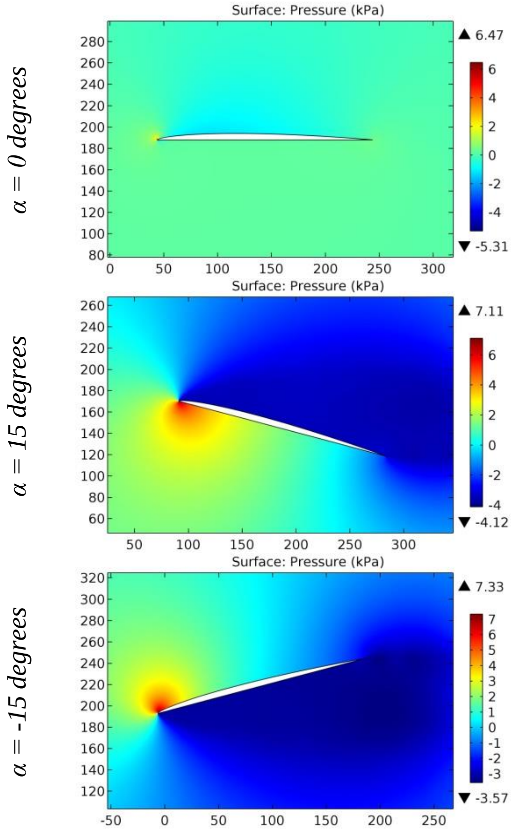

Figure 60. The pressure contours on the surfaces of the SIMPLEX3 airfoil.

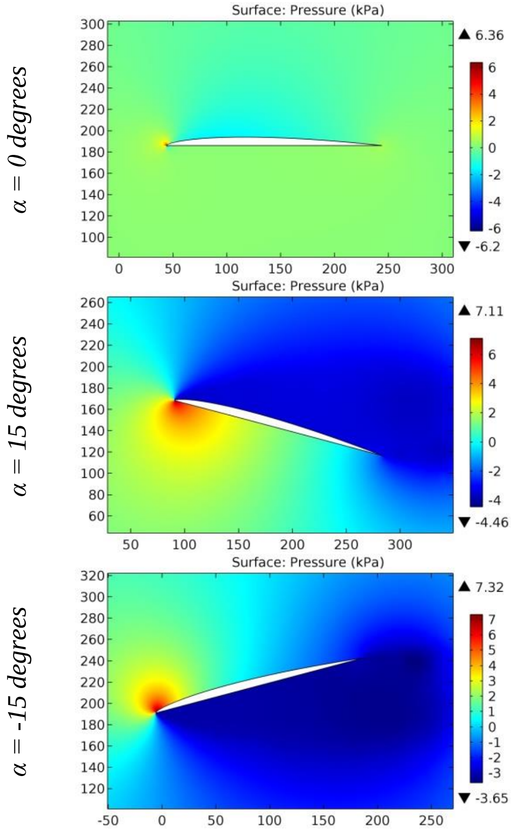

Figure 61. The pressure contours on the surfaces of the SIMPLEX4 airfoil.

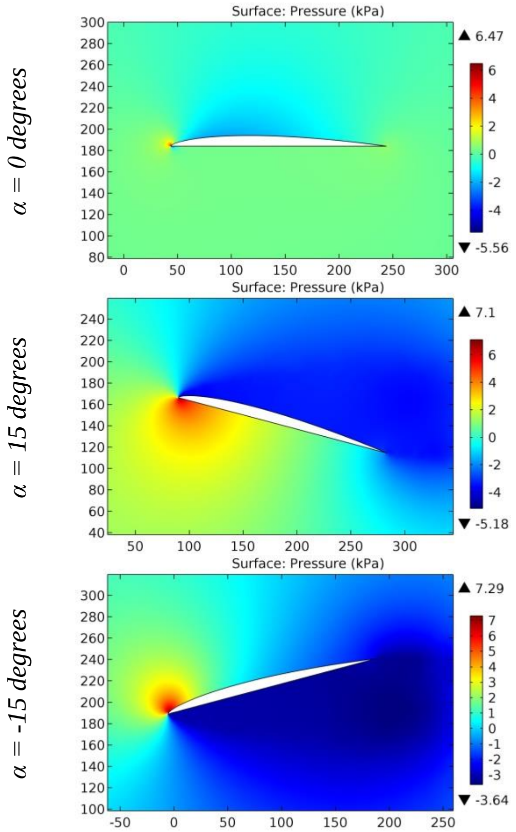

Figure 62. The pressure contours on the surfaces of the SIMPLEX5 airfoil.

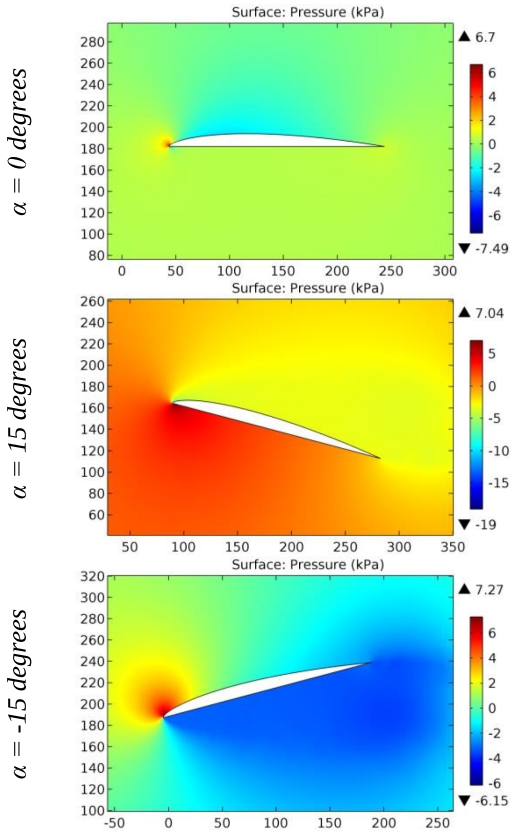

Figure 63. The pressure contours on the surfaces of the SIMPLEX6 airfoil.

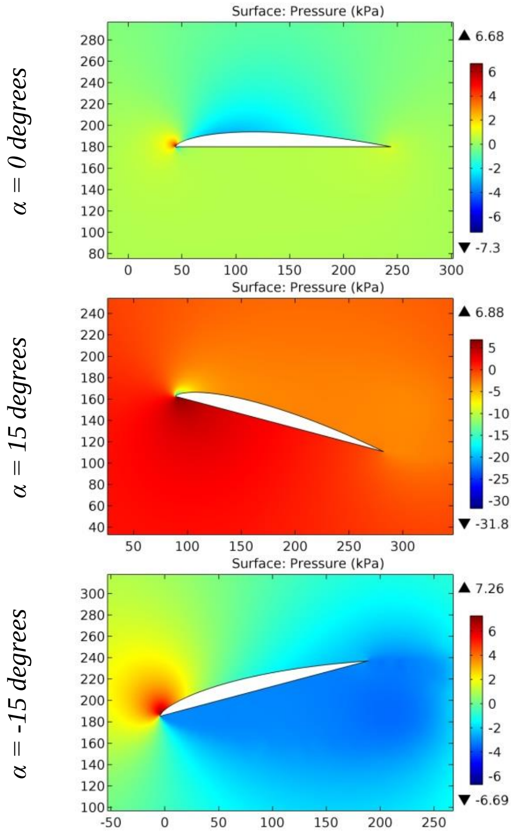

Figure 64. The pressure contours on the surfaces of the SIMPLEX7 airfoil.

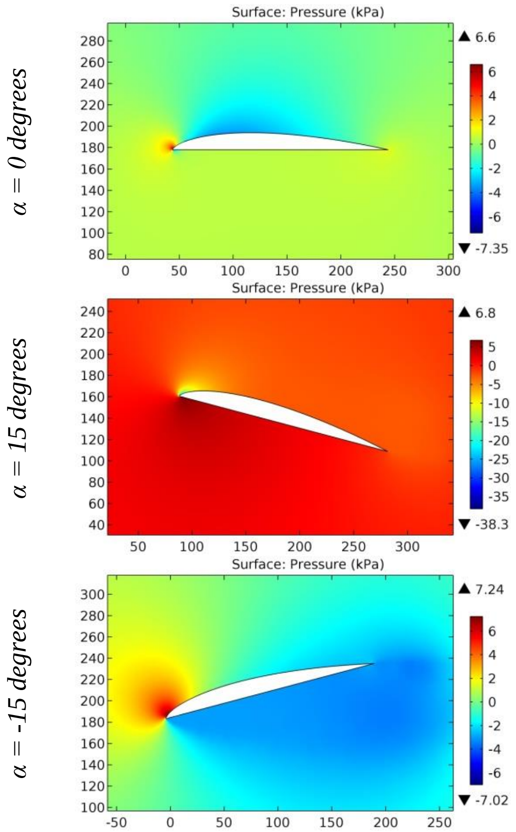

Figure 65. The pressure contours on the surfaces of the SIMPLEX8 airfoil.

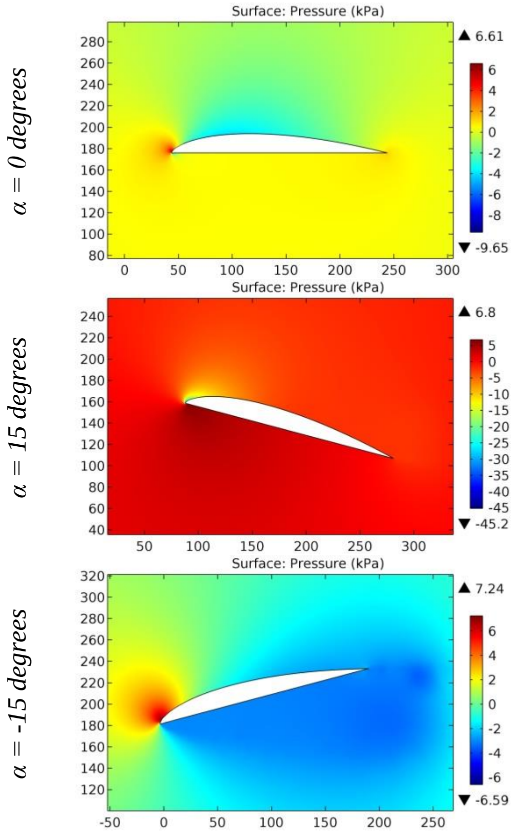

Figure 66. The pressure contours on the surfaces of the SIMPLEX9 airfoil.

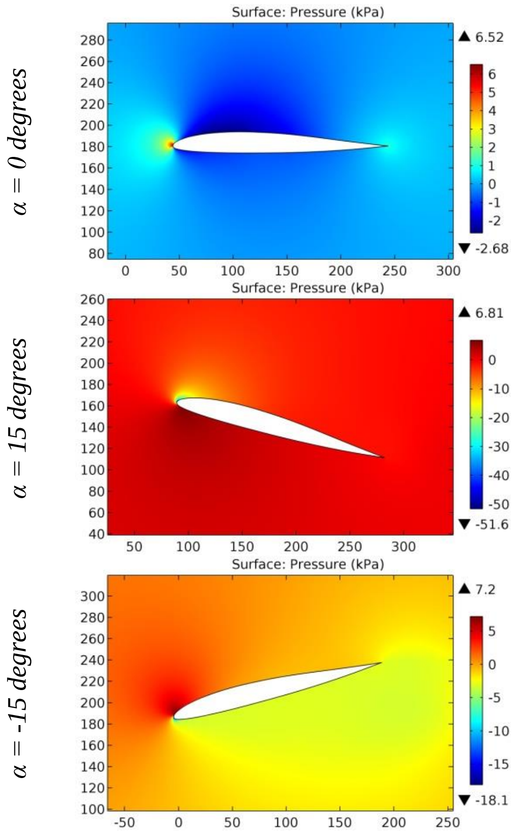

Figure 67. The pressure contours on the surfaces of the Sipkill 1,7/10 airfoil.

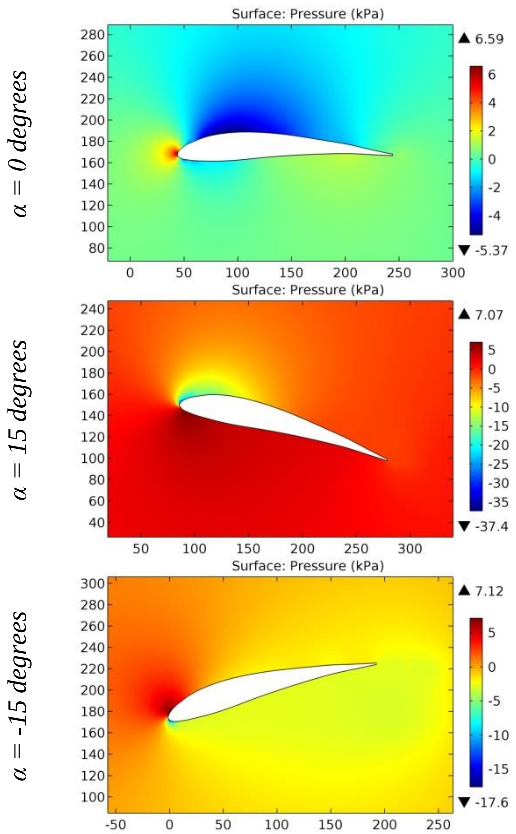

Figure 68. The pressure contours on the surfaces of the SL 1 airfoil.

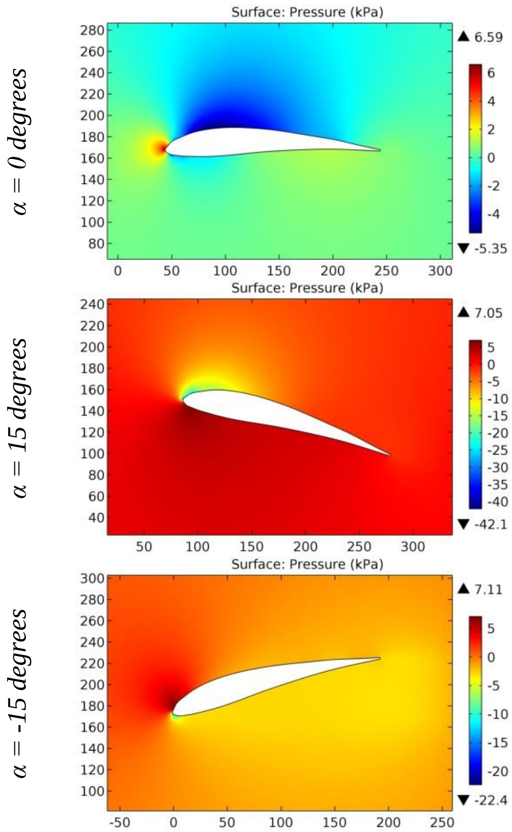

Figure 69. The pressure contours on the surfaces of the SL-1 airfoil.

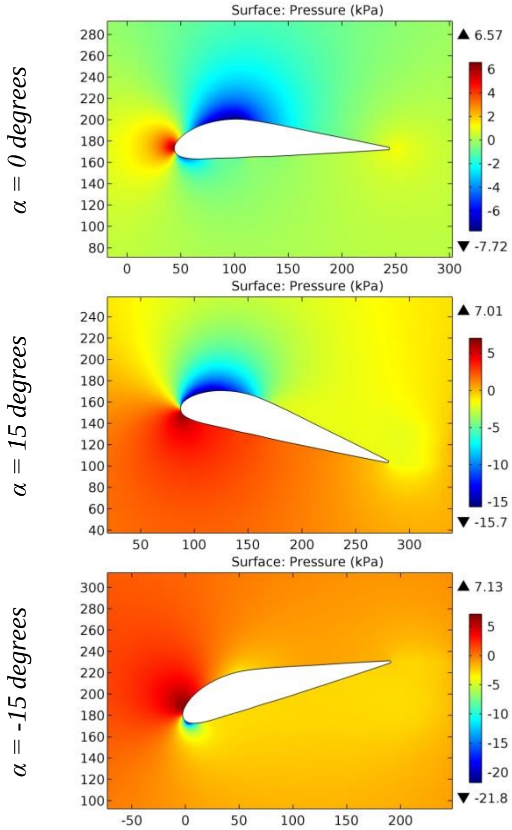

Figure 70. The pressure contours on the surfaces of the SLOTFLAP airfoil.

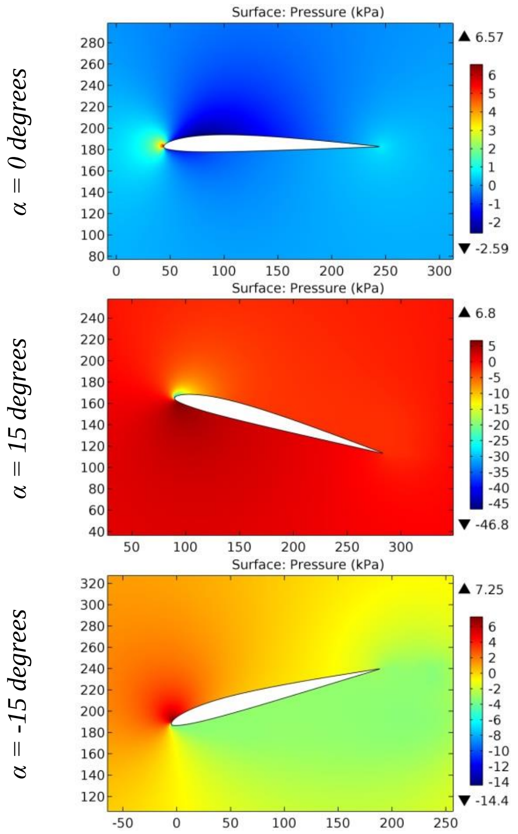

Figure 71. The pressure contours on the surfaces of the SM8016m airfoil.

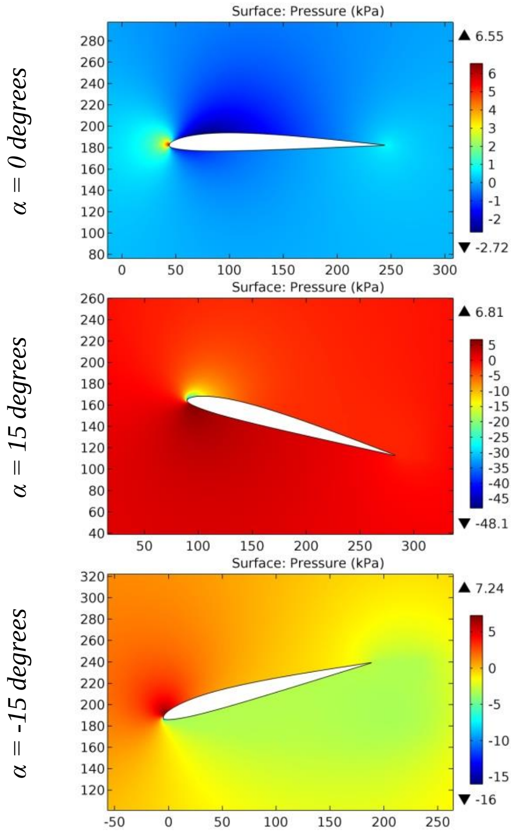

Figure 72. The pressure contours on the surfaces of the SM8516m airfoil.

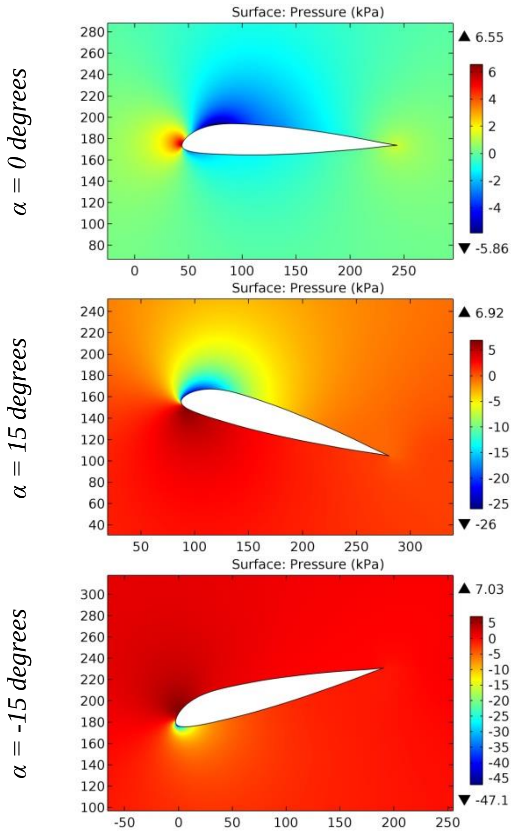

Figure 73. The pressure contours on the surfaces of the Smoothed ATR airfoil coordinates obtained using A.

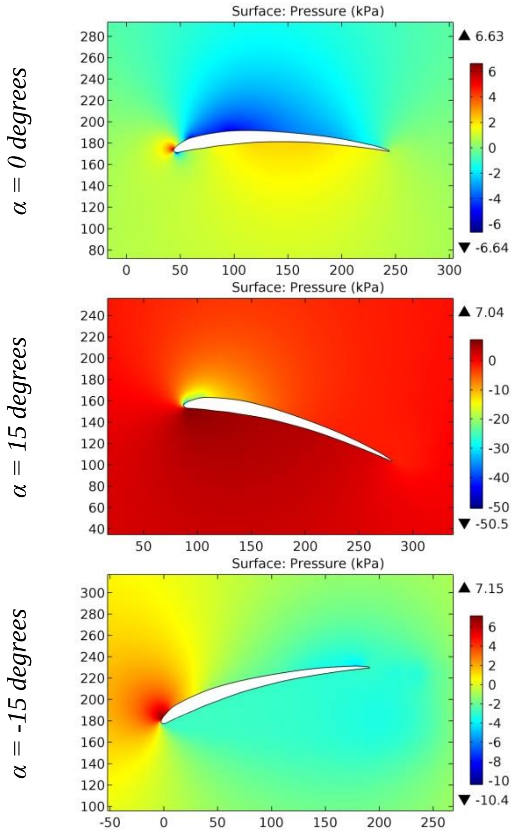

Figure 74. The pressure contours on the surfaces of the SOAVE-61 airfoil.

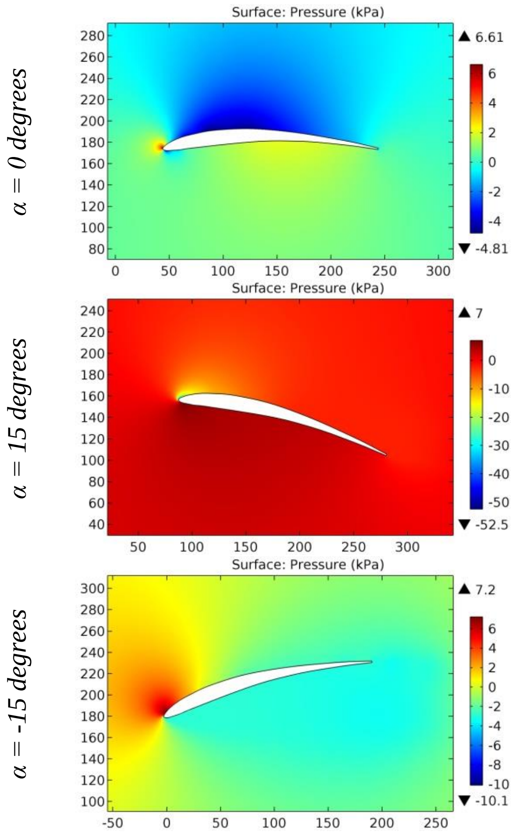

Figure 75. The pressure contours on the surfaces of the SOKOLOV airfoil.

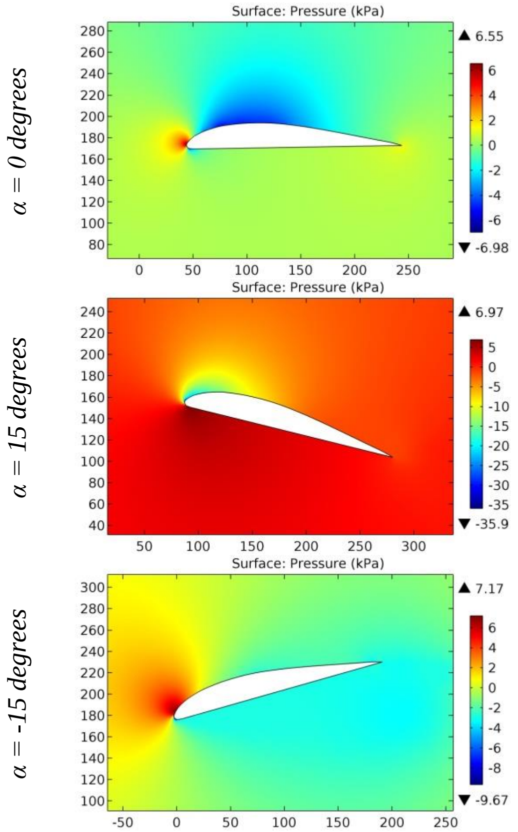

Figure 76. The pressure contours on the surfaces of the SPICA airfoil.

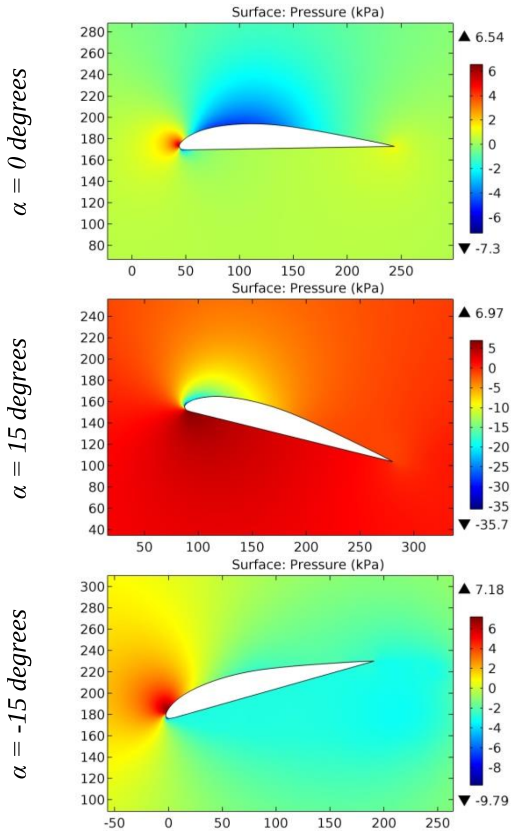

Figure 77. The pressure contours on the surfaces of the SPICA 11,73% smoothed airfoil.

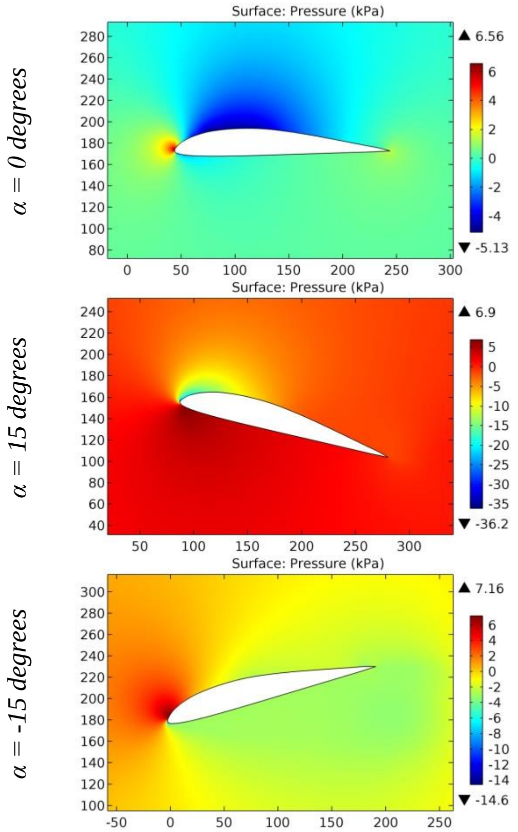

Figure 78. The pressure contours on the surfaces of the SPICAM1 airfoil.

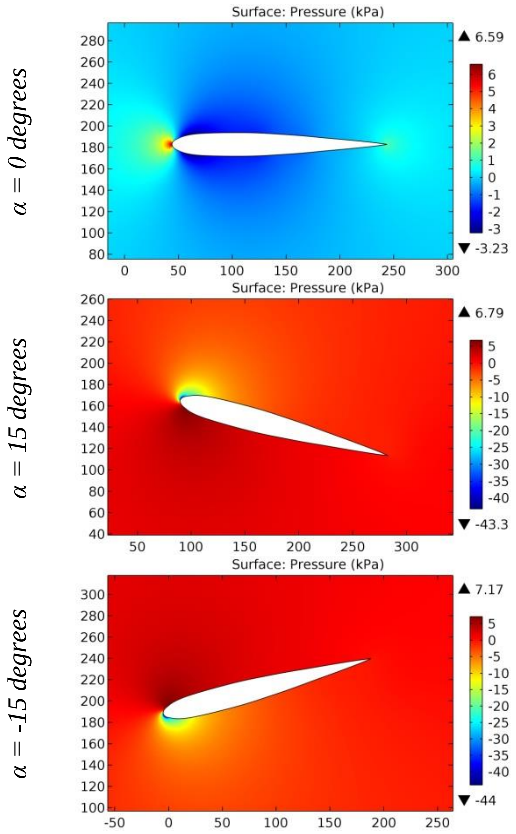

Figure 79. The pressure contours on the surfaces of the ST CYR 171 (ROYER) airfoil.

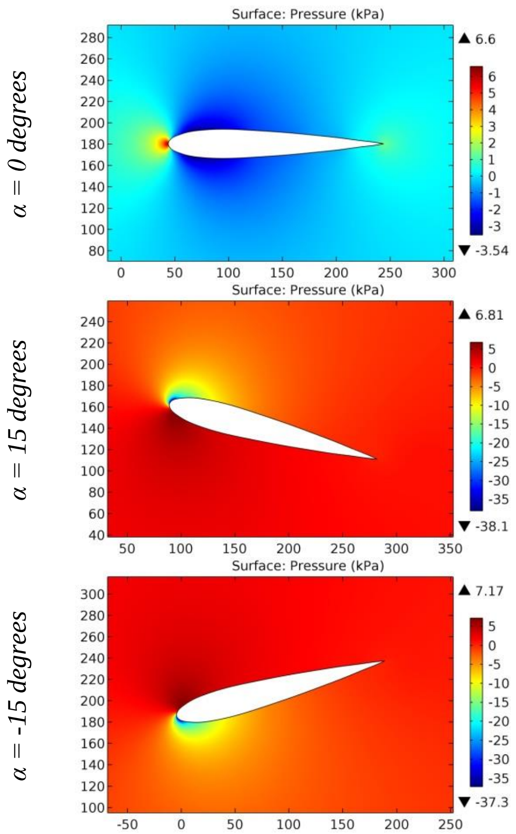

Figure 80. The pressure contours on the surfaces of the ST CYR 172 (ROYER) airfoil.

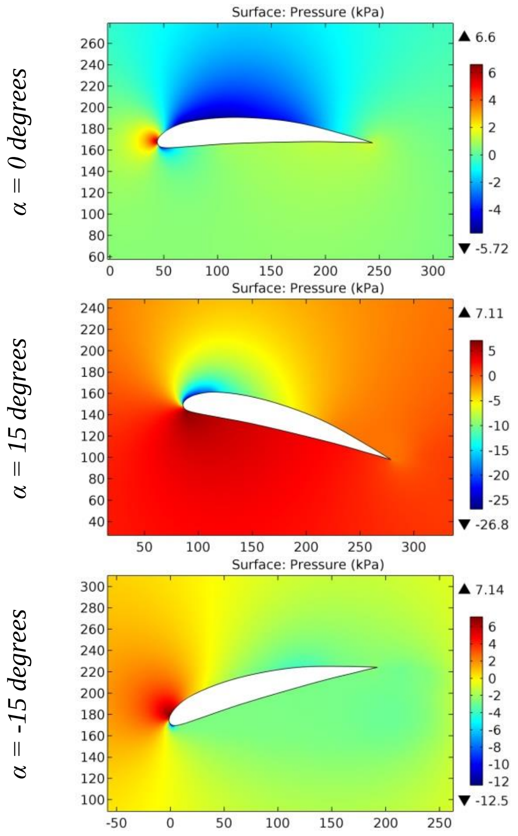

Figure 81. The pressure contours on the surfaces of the ST CYR 24 airfoil.

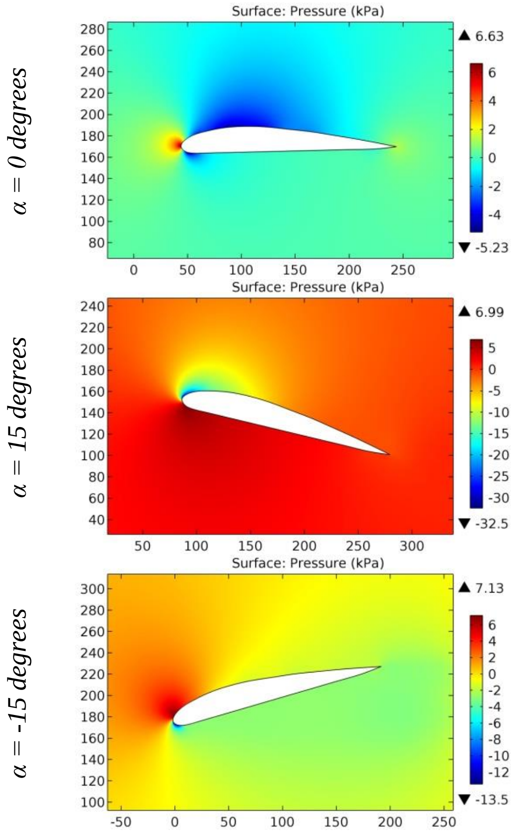

Figure 82. The pressure contours on the surfaces of the STCYR117 airfoil.

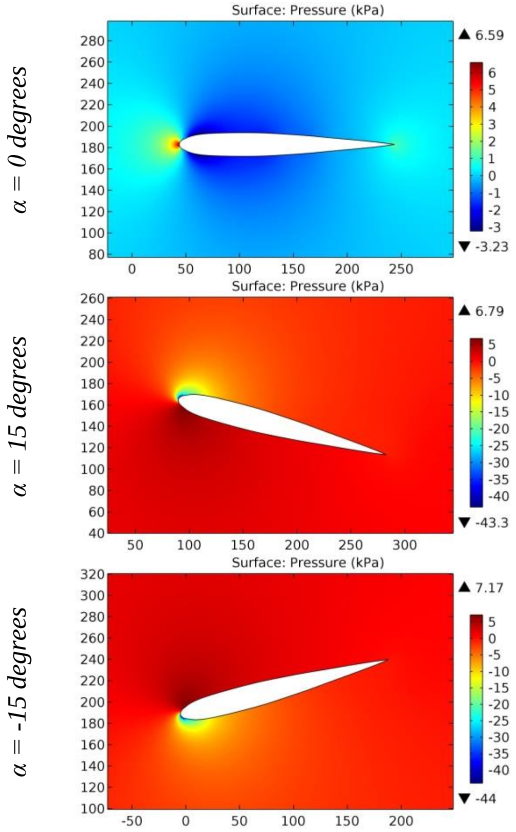

Figure 83. The pressure contours on the surfaces of the STCYR171 airfoil.

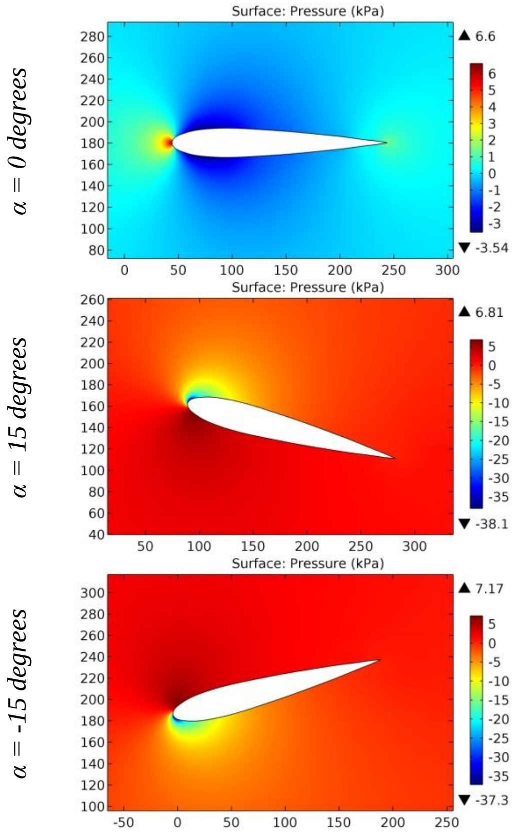

Figure 84. The pressure contours on the surfaces of the STCYR172 airfoil.

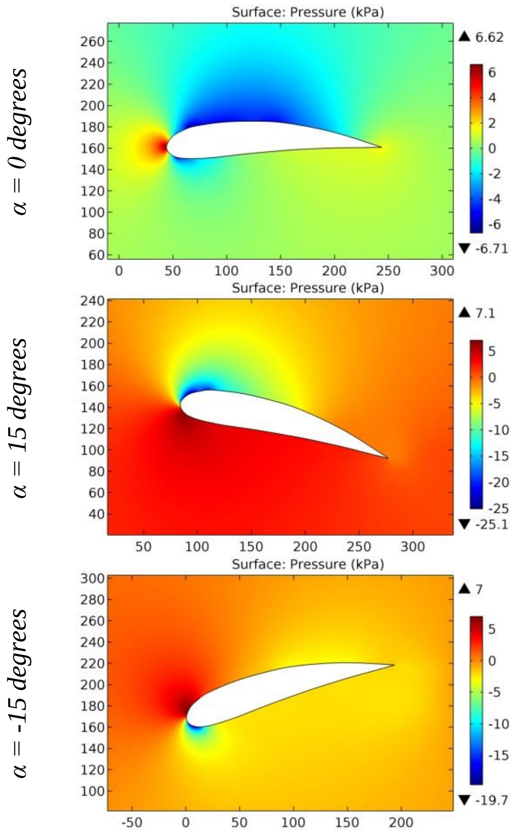

Figure 85. The pressure contours on the surfaces of the STCYR234 airfoil.

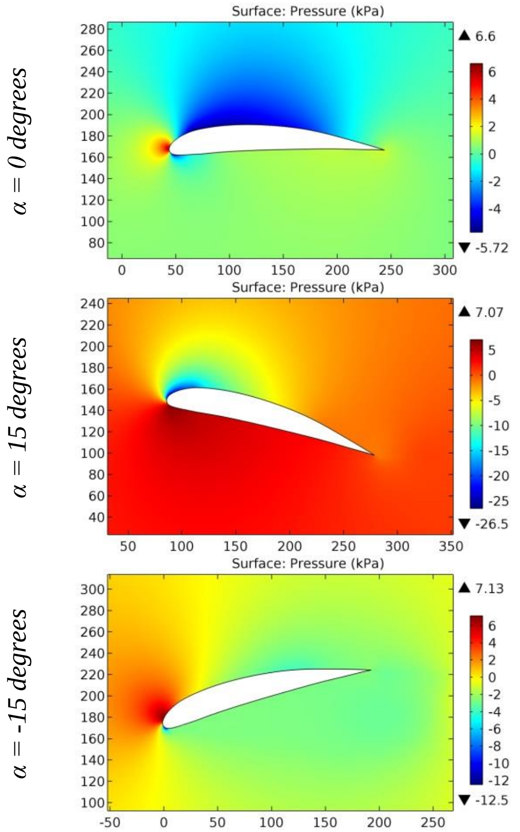

Figure 86. The pressure contours on the surfaces of the STCYR-24 airfoil.

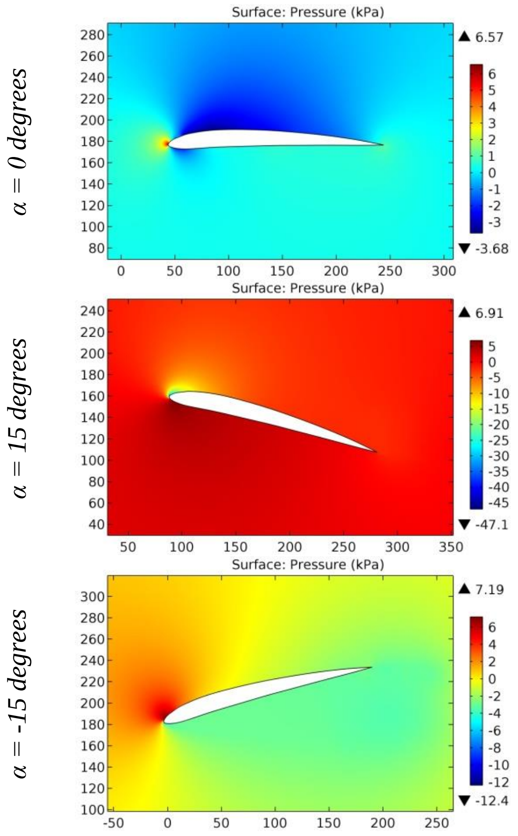

Figure 87. The pressure contours on the surfaces of the STCYR-34 airfoil.

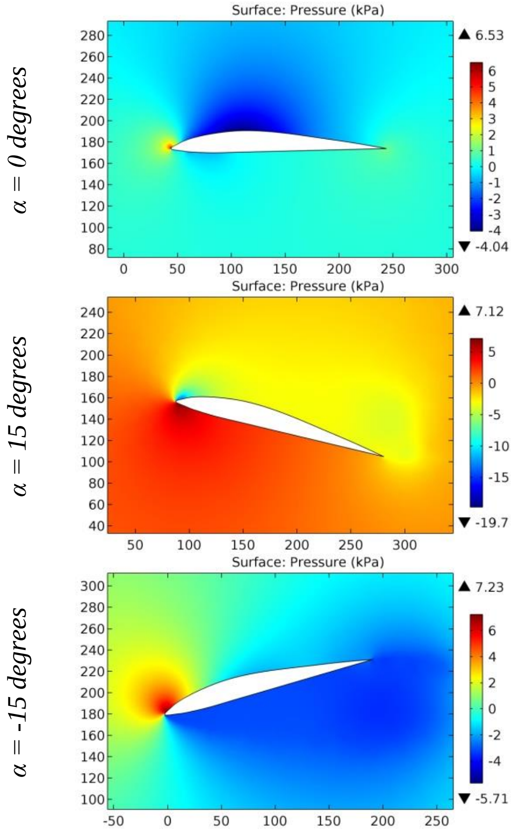

Figure 88. The pressure contours on the surfaces of the STCYR-52 airfoil.

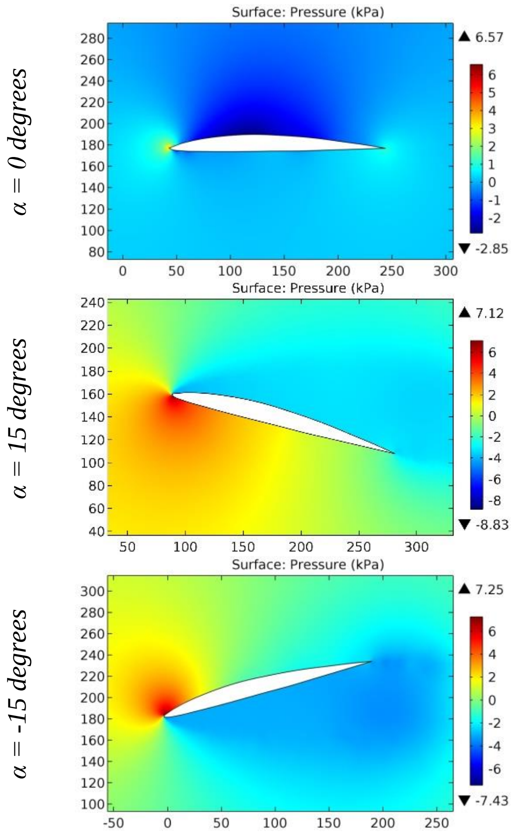

Figure 89. The pressure contours on the surfaces of the STCYR-53 airfoil.

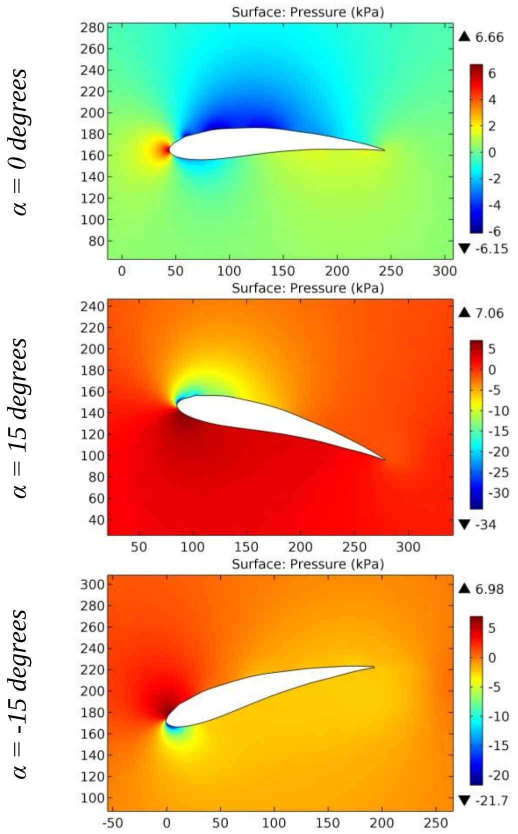

Figure 90. The pressure contours on the surfaces of the STCYR-56 airfoil.

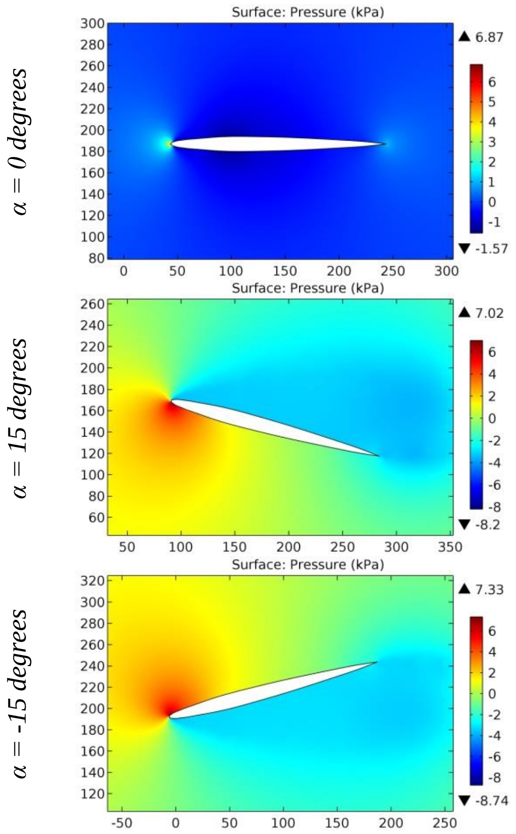

Figure 91. The pressure contours on the surfaces of the STCYR-58 airfoil.

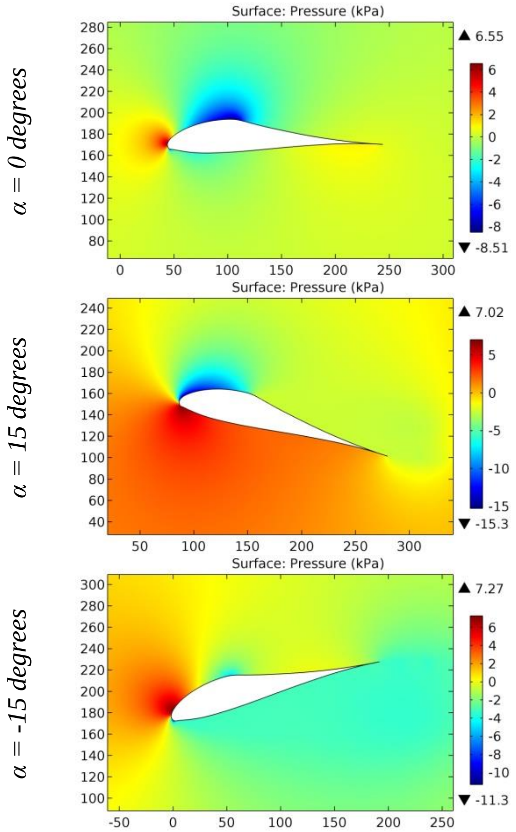

Figure 92. The pressure contours on the surfaces of the STRAND airfoil.

The size of the leading edge radius of the airfoil affects the drag coefficient. The design of the airplane experiences the least stress due to the smaller contact area of the surfaces with air flows at zero angle of attack. The lowest drag is observed during the horizontal flight of the airplane with the SIMPLEX1 wing profile, and the greatest drag is observed during the horizontal flight of the airplane with the STCYR-58 wing profile. These calculated pressure values differ slightly in the conditions of subsonic flight of the airplane. It is also determined that the SC(2)-0714 Supercritical and SI-63008 airfoils are subjected to greater pressure during the climb maneuver of the airplane, and the remaining airfoils are subjected to greater pressure during the descent maneuver of the airplane. The greatest pressure drop was determined on the surfaces of the SI-63008 airfoil during maneuvers. Negative pressure is formed on the surface of the SIMPLEX1 airfoil hidden from the movement of air flow during maneuvers. This thin airfoil is characterized by the lower drag during the horizontal flight of the airplane, and the greater drag during maneuvers. This is true for the airfoils selected for analysis.

Conclusion

The aerodynamic characteristics of the airplane wing can be improved by increasing the lift and reducing the drag. It is noted that the variable radius of the leading edge, turning into the convex upper or lower surfaces of the airfoil, helps to reduce the effective pressure on the wing during the descent maneuver of the airplane. The STCYR-56 airfoil is characterized by a decrease in positive pressure on the leading edge during the airplane descent, compared with the effective pressure during the airplane climb.

References:

1. Anderson, J. D. (2010). *Fundamentals of Aerodynamics*. McGraw-Hill, Fifth edition.
2. Shevell, R. S. (1989). *Fundamentals of Flight.* Prentice Hall, Second edition.
3. Houghton, E. L., & Carpenter, P. W. (2003). *Aerodynamics for Engineering Students*. Fifth edition, Elsevier.
4. Lan, E. C. T., & Roskam, J. (2003). *Airplane Aerodynamics and Performance.* DAR Corp.
5. Sadraey, M. (2009). *Aircraft Performance Analysis.* VDM Verlag Dr. Müller.
6. Anderson, J. D. (1999). *Aircraft Performance and Design*. McGraw-Hill.
7. Roskam, J. (2007). *Airplane Flight Dynamics and Automatic Flight Control*, Part I. DAR Corp.
8. Etkin, B., & Reid, L. D. (1996). *Dynamics of Flight, Stability and Control.* Third Edition, Wiley.
9. Stevens, B. L., & Lewis, F. L. (2003). *Aircraft Control and Simulation*. Second Edition, Wiley.
10. Chemezov, D., et al. (2021). Pressure distribution on the surfaces of the NACA 0012 airfoil under conditions of changing the angle of attack. *ISJ Theoretical & Applied Science, 09 (101)*, 601-606.
11. Chemezov, D., et al. (2021). Stressed state of surfaces of the NACA 0012 airfoil at high angles of attack. *ISJ Theoretical & Applied Science, 10 (102)*, 601-604.
12. Chemezov, D., et al. (2021). Reference data of pressure distribution on the surfaces of airfoils having the names beginning with the letter A (the first part). *ISJ Theoretical & Applied Science, 10 (102)*, 943-958.
13. Chemezov, D., et al. (2021). Reference data of pressure distribution on the surfaces of airfoils having the names beginning with the letter A (the second part). *ISJ Theoretical & Applied Science, 11 (103)*, 656-675.
14. Chemezov, D., et al. (2021). Reference data of pressure distribution on the surfaces of airfoils having the names beginning with the letter B. *ISJ Theoretical & Applied Science, 11 (103)*, 1001-1076.
15. Chemezov, D., et al. (2021). Reference data of pressure distribution on the surfaces of airfoils having the names beginning with the letter C. *ISJ Theoretical & Applied Science, 12 (104)*, 814-844.
16. Chemezov, D., et al. (2021). Reference data of pressure distribution on the surfaces of airfoils having the names beginning with the letter D. *ISJ Theoretical & Applied Science, 12 (104)*, 1244-1274.
17. Chemezov, D., et al. (2022). Reference data of pressure distribution on the surfaces of airfoils (hydrofoils) having the names beginning with the letter E (the first part). *ISJ Theoretical & Applied Science, 01 (105)*, 501-569.
18. Chemezov, D., et al. (2022). Reference data of pressure distribution on the surfaces of airfoils (hydrofoils) having the names beginning with the letter E (the second part). *ISJ Theoretical & Applied Science, 01 (105)*, 601-671.

19. Chemezov, D., et al. (2022). Reference data of pressure distribution on the surfaces of airfoils having the names beginning with the letter F. *ISJ Theoretical & Applied Science, 02 (106)*, 101-135.
20. Chemezov, D., et al. (2022). Reference data of pressure distribution on the surfaces of airfoils having the names beginning with the letter G (the first part). *ISJ Theoretical & Applied Science, 03 (107)*, 701-784.
21. Chemezov, D., et al. (2022). Reference data of pressure distribution on the surfaces of airfoils having the names beginning with the letter G (the second part). *ISJ Theoretical & Applied Science, 03 (107)*, 901-984.
22. Chemezov, D., et al. (2022). Reference data of pressure distribution on the surfaces of airfoils having the names beginning with the letter G (the third part). *ISJ Theoretical & Applied Science, 04 (108)*, 401-484.
23. Chemezov, D., et al. (2022). Reference data of pressure distribution on the surfaces of airfoils having the names beginning with the letter H (the first part). *ISJ Theoretical & Applied Science, 05 (109)*, 201-258.
24. Chemezov, D., et al. (2022). Reference data of pressure distribution on the surfaces of airfoils having the names beginning with the letter H (the second part). *ISJ Theoretical & Applied Science, 05 (109)*, 529-586.
25. Chemezov, D., et al. (2022). Reference data of pressure distribution on the surfaces of airfoils having the names beginning with the letter I. *ISJ Theoretical & Applied Science, 06 (110)*, 1-7.
26. Chemezov, D., et al. (2022). Reference data of pressure distribution on the surfaces of airfoils having the names beginning with the letter J. *ISJ Theoretical & Applied Science, 06 (110)*, 18-25.
27. Chemezov, D., et al. (2022). Reference data of pressure distribution on the surfaces of airfoils having the names beginning with the letter K. *ISJ Theoretical & Applied Science, 07 (111)*, 1-10.
28. Chemezov, D., et al. (2022). Reference data of pressure distribution on the surfaces of airfoils having the names beginning with the letter L. *ISJ Theoretical & Applied Science, 07 (111)*, 101-118.
29. Chemezov, D., et al. (2022). Reference data of pressure distribution on the surfaces of airfoils having the names beginning with the letter M. *ISJ Theoretical & Applied Science, 10 (114)*, 307-392.
30. Chemezov, D., et al. (2022). Reference data of pressure distribution on the surfaces of airfoils having the names beginning with the letter N (the first part). *ISJ Theoretical & Applied Science, 12 (116)*, 801-892.
31. Chemezov, D., et al. (2022). Reference data of pressure distribution on the surfaces of airfoils having the names beginning with the letter N (the second part). *ISJ Theoretical & Applied Science, 12 (116)*, 901-990.
32. Chemezov, D., et al. (2023). Reference data of pressure distribution on the surfaces of airfoils having the names beginning with the letter O. *ISJ Theoretical & Applied Science, 01 (117)*, 624-635.
33. Chemezov, D., et al. (2023). Reference data of pressure distribution on the surfaces of airfoils having the names beginning with the letter P. *ISJ Theoretical & Applied Science, 02 (118)*, 48-61.
34. Chemezov, D., et al. (2023). Reference data of pressure distribution on the surfaces of airfoils having the names beginning with the letter R. *ISJ Theoretical & Applied Science, 03 (119)*, 104-165.